

SPECTROSCOPY

europa

Informing European spectroscopists for over 40 years

Built Heritage in marine environments
Micro FT-IR mapping and earthworms
IR QC of Chinese traditional medicine

WILEY

imp
implications



UltraCOOL Probe

- For maximum sensitivity
- 800 and 600MHz
 - 5mm C-H and H-X type
- ^{13}C : > x5 higher sensitivity
- ^1H : > x4 higher sensitivity

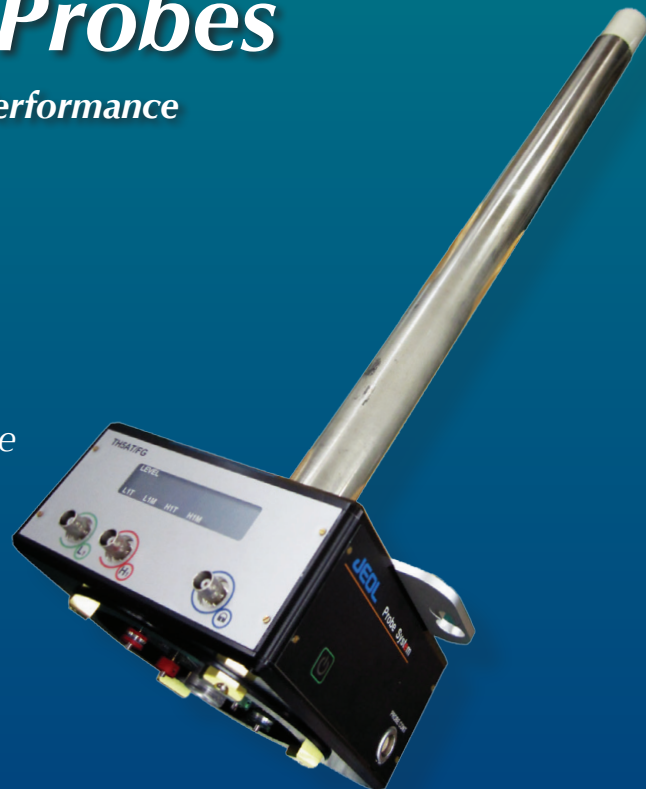


JEOL - NMR Probes

Advanced Technology and Performance

The SuperCOOL probe

- Low cost nitrogen cooled probe
- 400MHz 5mm tunable type
- ^{13}C : x3 higher sensitivity
- ^1H : > x3 higher sensitivity



Living by the sea has many benefits, but also brings problems, not least the corrosive effect of the air. My first house was about 20m from the sea, and the windows required frequent repainting and one side of the car rusted far more quickly than the other. However, the views were fantastic! The first article in this issue by Héctor Morillas, Maite Maguregui and Juan Manuel Madariaga is on "Spectroscopic evidences to understand the influence of marine environments on Built Heritage" and it looks at the use of Raman and XRF spectroscopies to investigate the different deterioration processes caused by marine aerosols. These techniques can detect the decay compounds and the original composition of the different materials from historical buildings close to the sea, which can then be used to explain the reactions that take place on them. This helps in the development of remedial actions and preventive conservation strategies for historical buildings.

Earthworm secretions are of interest to Mark Hodson, Liane Benning, Gianfelice Cinque, Bea Demarchi, Mark

Frogley, Kirsty Penkman, Juan Rodriguez-Blanco, Paul Schofield, Emma Versteegh and Katia Wehbe in "Synchrotron-based micro Fourier transform infrared mapping to investigate the spatial distribution of amorphous and crystalline calcium carbonate in earthworm-secreted calcium carbonate balls". Several earthworm species secrete very small granules of calcium carbonate, and the authors think these are involved in pH regulation. These granules contain different polymorphs of calcium carbonate, including the amorphous form which is very unstable in the laboratory. To investigate this they have FT-IR spectroscopy and mapping, and are continuing this work with Ca XANES.

Christian Huck and co-authors look at "Infrared spectroscopic techniques for the non-invasive and rapid quality control of Chinese traditional medicine Si-Wu-Tang". They have used benchtop mid-IR and NIR as well as portable NIR instruments for quick and non-invasive quality control of this traditional Chinese medicine. Adulterations could be detected, as well as the raw herbs and different

sources of the Si-Wu-Tang. The success of the mobile NIR instrument is particularly interesting due to the growing interest in such technology for its ease-of-use and cost.

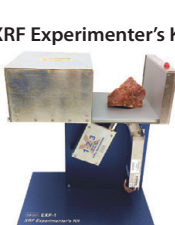
In their Sampling Column, Kim Esbensen and Claas Wagner stray into Quality Matters territory as they look at standards and how they work with the Theory of Sampling. Kim and Claas are concerned that many international standards do not comply with the TOS and that this compromises the results.

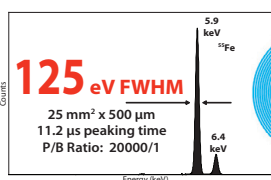
In the last issue, I reported on many new products introduced at Pittcon. This time, I've been to Analytica in Munich, Germany. Whilst many of the new products there had already been seen at Pittcon (and so are not included again), there was still plenty of new instrumentation. We also have a short New Products section and a Product Focus on Imaging Spectroscopy.

La Michael

Silicon Drift Detectors

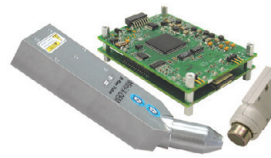
XRF Experimenter's Kit





125 eV FWHM
25 mm² x 500 μm
11.2 μs peaking time
P/B Ratio: 20000/1


OEM Components



NEW!! FAST SDD®

Count Rate >1,000,000 CPS


Complete X-Ray Spectrometer

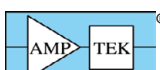



OEM's #1 Choice for XRF

www.amptek.com

XRF System





The sea can be a damaging environment for buildings. Find out how spectroscopy is being used to understand the mechanisms causing damage and to develop conservation strategies in the article starting on page 6.

Publisher

Ian Michael
E-mail: ian@impublications.com

Article Editor

John Chalmers
VSConsulting, Stokesley, UK.
E-mail: johnmchalmers@aol.com

Advertising Sales UK and Ireland

Ian Michael
IM Publications, 6 Charlton Mill,
Charlton, Chichester, West Sussex PO18 0HY,
United Kingdom. Tel: +44-1243-811334,
Fax: +44-1243-811711,
E-mail: ian@impublications.com.

Americas

Joe Tomaszewski
John Wiley & Sons Inc.
Tel: +1-908-514-0776
E: jtomaszews@wiley.com

Europe and the Rest of World

Stephen Parkes and Charlotte Redfern
John Wiley & Sons Ltd, The Atrium, Southern Gate,
Chichester, West Sussex PO19 8SQ, UK,
Tel: +44-1243-770367, Fax: +44-1243-770432,
E-mail: stephen.parkes@wiley.com and
credferm@wiley.com

Paid subscriptions

Journals Subscriptions Department, John Wiley &
Sons, Ltd, The Atrium, Southern Gate, Chichester,
West Sussex PO19 8SQ, UK.
Tel +44-1243 779777, Fax +44-1243 843232,
e-mail: cs-journals@wiley.co.uk

Spectroscopy Europe is a joint publication of
John Wiley & Sons Ltd, The Atrium, Southern
Gate, Chichester, West Sussex PO19 8SQ, UK,
and IM Publications LLP, 6 Charlton Mill, Charlton,
Chichester, West Sussex PO18 0HY, UK.

Vol. 28 No. 3
June/July 2016

ISSN 0966-0941

CONTENTS

3 Editorial

6 Spectroscopic evidences to understand the influence of marine environments on Built Heritage

Héctor Morillas, Maite Maguregui and Juan Manuel Madariaga

12 Synchrotron-based micro Fourier transform infrared mapping to investigate the spatial distribution of amorphous and crystalline calcium carbonate in earthworm-secreted calcium carbonate balls

Mark E. Hodson, Liane G. Benning, Gianfelice Cinque, Bea Demarchi, Mark Frogley, Kirsty E.H. Penkman, Juan D. Rodriguez-Blanco, Paul F. Schofield, Emma A.A. Versteegh and Katia Wehbe

16 Infrared spectroscopic techniques for the non-invasive and rapid quality control of Chinese traditional medicine Si-Wu-Tang

C.K. Pezzei, M. Watschinger, V.A. Huck-Pezzei, C.B.S. Lau, Z. Zuo, P.C. Leung and C.W. Huck

22 Sampling Column

There are standards—and there is *the* standard

28 Analytica report 2016

Ian Michael

31 Product Focus

Imaging Spectroscopy

32 New Products

33 Diary

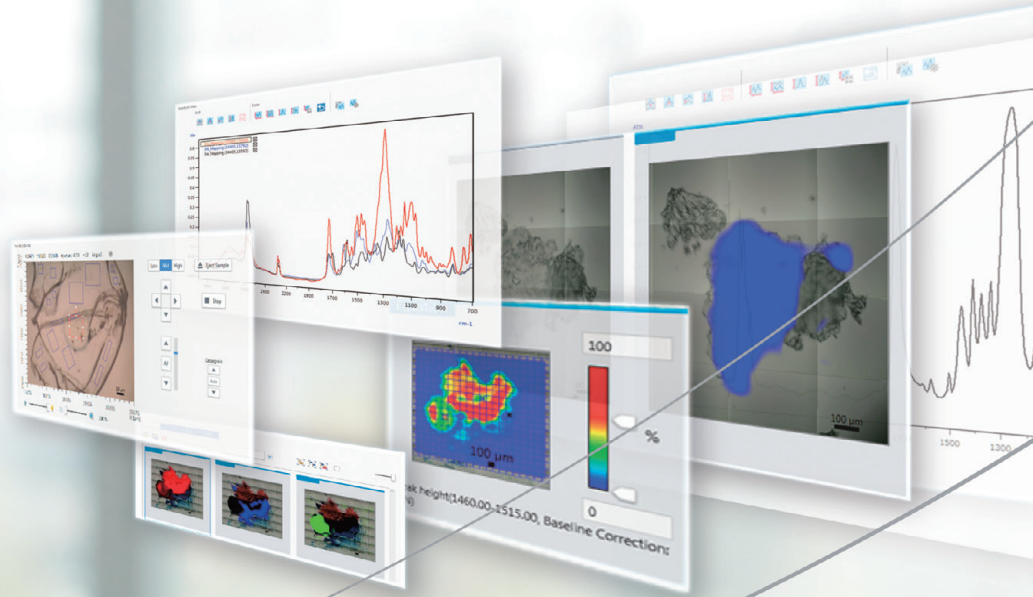
Spectroscopy Europe is a controlled circulation journal, published seven times a year and available free-of-charge to qualifying individuals in Europe. Others can subscribe at the rate of €152 (Europe), £108 (UK), \$208 (ROW, postage included) for the seven issues published in 2016. All paid subscription enquiries should be addressed to: *Spectroscopy Europe*, John Wiley & Sons Ltd, Journals Administration Department, The Atrium, Southern Gate, Chichester, West Sussex PO19 8SQ, UK.

Copyright 2016 John Wiley & Sons Ltd and IM Publications LLP

All rights reserved. No part of this publication may be reproduced, stored in a retrieval system, or transmitted, in any form or by any means, electronic, mechanical, photocopying, recording or otherwise, without the prior permission of the publisher in writing.
Printed in the UK by Headley Brothers Ltd, Ashford, Kent.

WILEY

imp
implications



Unveiling the cause of failures

AIM-9000 Infrared Microscope System: quick and easy micro analysis

The AIM-9000 Infrared Microscope for automatic failure analysis delivers a unique concept for micro sample analysis – applicable for various industries. Its functionality is simpler and more convenient to use than ever before. A wide range of accessories complements the instrument to fully support sample observation, measurement and identification.

Highest sensitivity marketwide
with a signal-to-noise ratio of a staggering 30.000/1

Automatic zoom-in from eye-size to contaminant-size
through wide field camera feature

Automatic contaminant recognition function
sets aperture on measurement spots automatically

Automatic identification of the spectrum
through contaminant analysis program

www.shimadzu.eu/aim-9000



IRTracer-100 + AIM-9000



IRAffinity-1S + AIM-9000

Spectroscopic evidences to understand the influence of marine environments on Built Heritage

Héctor Morillas,^a Maite Maguregui^b and Juan Manuel Madariaga^a

^aDepartment of Analytical Chemistry, Faculty of Science and Technology, University of the Basque Country UPV/EHU, PO Box 644, 48080 Bilbao, Basque Country, Spain. E-mail: hector.morillas@ehu.es

^bDepartment of Analytical Chemistry, Faculty of Pharmacy, University of the Basque Country UPV/EHU, PO Box 450, 01080 Vitoria-Gasteiz, Basque Country, Spain

Introduction

Marine aerosols are chemically complex systems formed by inorganic salts and organic matter, together with airborne particulate matter from the surrounding environment. The primary particles transported in marine aerosols (PMA) can cause different chemical reactions in the atmosphere, promoting formation of so-called Secondary Marine Aerosol (SMA) particles.

These kinds of particles, together with the natural crustal or mineral particles and the metallic airborne particulate matter emitted by anthropogenic sources (road traffic, industry etc.), can be deposited on building materials from a specific construction following wet or dry deposition processes.^{1–3}

The interactions of the natural and anthropogenic stressors present in marine atmospheres with building materials immersed within these kinds of atmospheres result in the formation of different types of pathologies. Examples of this are the alveolisations or loss of material, which are the consequence of salts (marine aerosol) deposition/redissolution cycles on the surface of façades,⁴ or water infiltrations containing harmful ions,^{5–7} which can penetrate the pores of a material by capillarity, forming in some cases efflorescence. In other cases, biological patinas can be formed on the buildings'

materials, acting sometimes as protective or as degradation layers for the material itself.⁸ SO_x emissions can also promote decaying processes on limestones⁹ and carbonated sandstones.³ This acid gas can be deposited following a wet process causing the formation of new sulfates on the material. These compounds, more soluble than carbonates, can be washed out due to the rainwater effect promoting the loss of material. On the other side, dry attack results in the formation of the so-called "black crusts", a patina made up of gypsum (CaSO₄·2H₂O) in which atmospheric particulate matter (crustal and metallic particles, organic compounds, soot etc.) is trapped.

In this work, the usefulness of a non-invasive analytical methodology based on the application of molecular (Raman spectroscopy) and elemental (X-ray Fluorescence, XRF) spectroscopic techniques (both single point and imaging analysis) was tested to understand the negative influence exerted by marine environments (with or without the influence of urban–industrial activities) on the conservation state of building materials close to the sea.

Instrumentation

The molecular analysis was performed using three different Raman spectrometers, all of them with an excitation

laser of 785 nm: (a) a portable Raman spectrometer (innoRam, B&W Tek Inc., USA), (b) a Raman microprobe (RA100, Renishaw, UK) and (c) a confocal Raman microscope (inVia, Renishaw, UK) equipped with a 20× and 50× objectives.

For the elemental analyses, the M4 Tornado benchtop instrument (Bruker Nano GmbH, Berlin, Germany) was used, with single point and imaging analysis options, operated under vacuum and equipped with a micro-focus side window Rh tube (powered by a low-power HV generator working at a maximum voltage of 50 kV and at a maximum current of 700 μA) and implementing a mechanical collimator allowing one to acquire measurements under 1 mm lateral resolution.

Buildings object of studies

Two buildings located in marine environments were considered for this work. One, the Igueldo lighthouse (San Sebastian) with direct marine and diffuse influence from an urban–industrial area was studied. In this historical building, cementitious materials, bricks, limestones and gypsum plasters were analysed. The other study was of sandstones from La Galea Fortress (Getxo), a building with direct marine and direct influence of a nearby urban–industrial area.

Table 1. Summary of the characteristic Raman bands of some decay compounds identified in the building materials from the Igueldo Lighthouse and La Galea Fortress.

Decay compounds	Mineral name	Building materials	ν (cm ⁻¹)
CaSO ₄ ·½ H ₂ O	Bassanite	Bricks, sandstone, limestones, mortars, cements & gypsum plasters	429m, 487m, 627m, 668m, 1015vs, 1128m
CaSO ₄	Anhydrite type III	Bricks, sandstone, Limestones, mortars, cements & gypsum Plasters	420m, 490m, 630m, 673m, 1025vs, 1167m.
Na ₃ (SO ₄)(NO ₃)·H ₂ O	Darapskite	Gypsum plasters	472ww, 619w, 640w, 707w, 729w, 993s, 1059vs, 1084w, 1122ww, 1354w, 1416w.
Na ₄ Ca(SO ₄) ₃ ·H ₂ O	Eugsterite	Gypsum plasters	1084s, 1124s
K ₃ Na ₇ Mg ₂ (SO ₄) ₆ (NO ₃) ₂ ·6H ₂ O	Humberstonite	Gypsum plasters	184ww, 217m, 457ww, 611m, 632s, 722s, 1013vs, 1048vs, 1067s.
K ₂ Ca(SO ₄)·H ₂ O	Syngenite	Gypsum plasters	441s, 472m, 492w, 603m, 621m, 633m, 642m, 661m, 981vs, 1006vs, 1082m, 1119m, 1139w, 1165w.
K ₂ Ca ₂ Mg(SO ₄) ₄ ·2H ₂ O	Polyhalite	Gypsum plasters	236m, 438m, 465s, 623ww, 653m, 989vs, 1016vs, 1071m, 1093m, 1131m, 1165m.
CaNa ₂ (SO ₄) ₂	Glauberite	Gypsum plasters	453w, 471s, 485m, 619m, 624m, 636m, 644s, 1001vs, 1106w, 1139s, 1156m, 1169m
(NH ₄) ₂ SO ₄	Mascagnite	Sandstones, bricks	449m, 614w, 622w, 974vs, 1104ww, 1417ww.
CaSO ₄ ·2H ₂ O	Gypsum	Bricks, sandstone, limestones, mortars, cements & gypsum plasters	413m, 492m, 619m, 673m, 1008vs, 1132m.
K ₂ SO ₄	Arcanite	Limestones and sandstones	455m, 619m, 988vs, 1092w, 1103w, 1144ww.
Fe ₂ (SO ₄) ₃ ·9H ₂ O	(para)coquimbite	Mortars, limestones and sandstones	500m, 600w, 1025vs, 1094ww, 1176ww, 1197ww.
MgSO ₄ ·4H ₂ O	Starkeyite	Limestones and sandstones	147w, 232w, 312w, 462m, 613m, 1001vs, 1084ww, 1115ww, 1155ww, 1603ww.
MgSO ₄ ·6H ₂ O	Hexahydrate	Limestones and sandstones	249w, 361w, 442w, 464ww, 603w, 982vs, 1083ww, 1148ww.
MgSO ₄ ·7H ₂ O	Epsomite	Limestones and sandstones	362ww, 445w, 462w, 609w, 985vs, 1082ww, 1145ww.
BaSO ₄	Baryte	Limestones and sandstones	460s, 618m, 648m, 987vs, 990vs, 1084m, 1104m, 1141w, 1169m.
[Ca ₆ Al ₂ (OH) ₁₂ (SO ₄) ₃ ·26H ₂ O]	Ettringite	Cements	218w, 361ww, 448m, 544m, 648m, 857s, 890m, 986vs, 1061m.
Na ₂ SO ₄	Thenardite	Bricks, mortars, cements, limestones and sandstones	450w, 465w, 621m, 632m, 647m, 992vs, 1101m, 1132m, 1152m.
Na ₂ SO ₄ ·10H ₂ O	Mirabilite	Bricks, mortars, cements, limestones and sandstones	446w, 458w, 616m, 628m, 989vs, 1108m, 1120m, 1130m.
KNO ₃	Niter	Bricks mortars, limestones and sandstones	712w, 1342w, 1357w, 1048vs, 1777ww.
Ca(NO ₃) ₂ ·4H ₂ O	Nitrocalcite	Bricks, mortars, limestones and sandstones	719w, 745w, 1048vs, 1352w, 1437m, 1640ww.
NaNO ₃	Nitratine	Bricks, mortars, limestones and sandstones	188m, 414ww, 518ww, 533ww, 722s, 1067vs, 1383w, 1663ww, 1775ww.
Ba(NO ₃) ₂	Nitrobarite	Limestones and sandstones	200w, 731m, 1025ww, 1046vs, 1402ww, 1631ww,
Mg(NO ₃) ₂	Nitromagnesite	Cements, limestones and sandstones	729s, 1059vs, 1359m, 1432w.
NH ₄ NO ₃	Nitrammite	Limestones and sandstones	714s, 1040vs, 1288w, 1412w, 1464w, 1654m.

vs, very strong; s, strong; m, medium; w, weak.

Analytical approach

First, an *in situ* screening of the aforementioned building materials was performed using a portable Raman spectrometer in order to extract prelim-

inary results. After that, samples were extracted from selected areas and they were analysed in-depth in the laboratory using micro-Raman spectroscopy and energy-dispersive-XRF (ED-XRF).

Results and discussion

The different decay compounds detected by Raman spectroscopy in the building materials from Igueldo Lighthouse and La Galea Fortress are summarised in Table 1. These

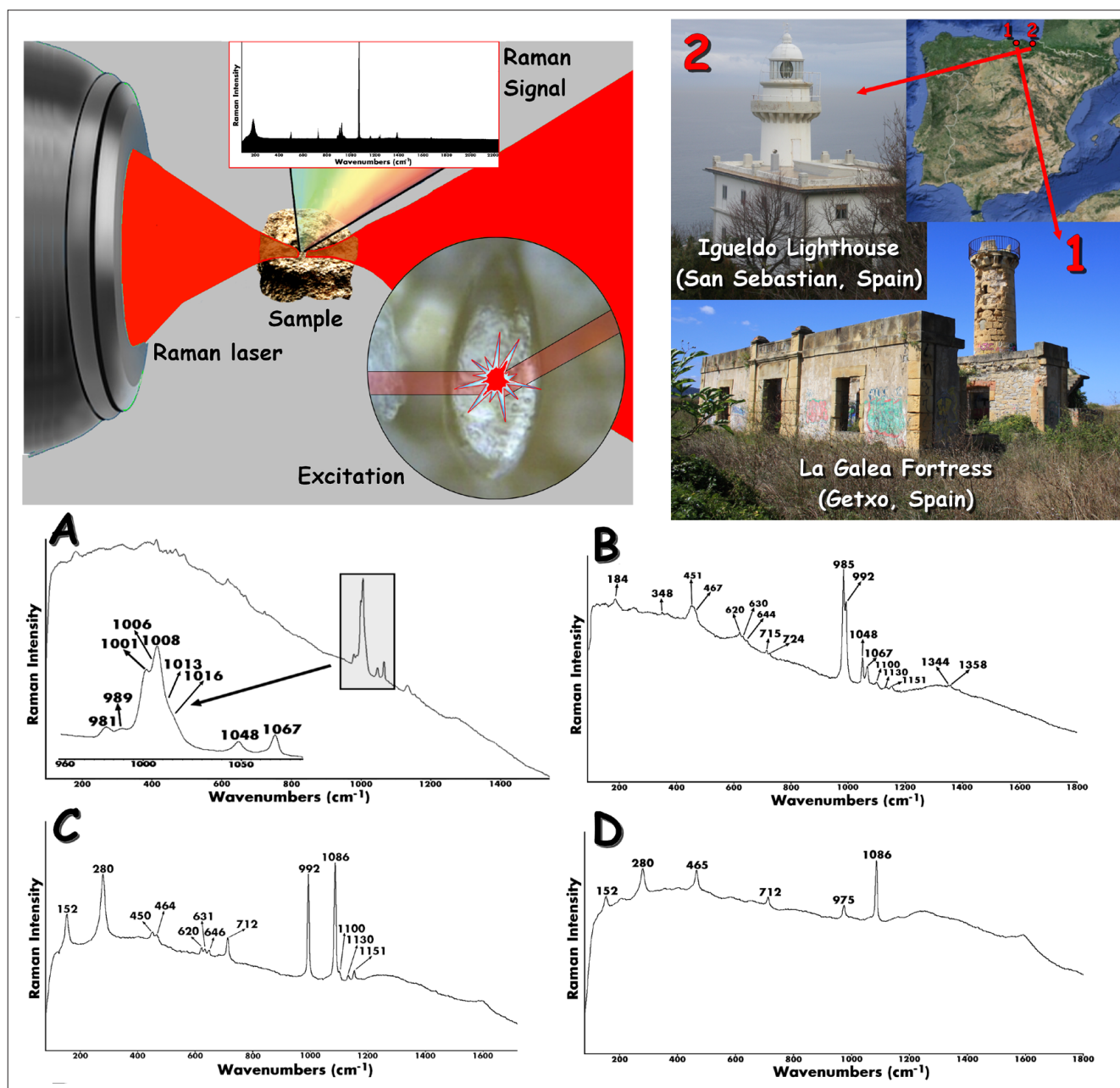


Figure 1. Representation of a sample being analysed by Raman spectroscopy (top-left) and Igueldo Lighthouse and La Galea Fortress as building objects of study (top-right). (A) main Raman bands of gypsum, syngenite, glauberite, polyhalite and humberstonite on gypsum plasters from Igueldo Lighthouse; (B) main Raman bands of nitratine, niter, thenardite and epsomite on sandstone from La Galea Fortress; (C) main Raman bands of thenardite and calcite on sandstone from La Galea Fortress; and (D) main Raman bands of mascagnite and calcite on sandstone from La Galea Fortress.

compounds were formed by chemical reactions between the emissions and/or infiltration waters coming from both surrounding environments and the original compounds in the respective materials of the two buildings. In this sense, the formation of detected sulfates, nitrates and mixed sulfates–nitrates can only be explained by the reactivity between the

wet deposition of atmospheric gaseous acids (CO_2 , SO_2 and NO_x) on the carbonate compounds present in the original materials.

It is important to highlight that the combination of different molecular analysis techniques is necessary in order to confirm and complement the results obtained with only one analytical tech-

nique. In this sense, the combination of Raman spectroscopy and X-ray Diffraction is a good strategy to obtain complete molecular information. In some cases, if the analysed matrix is complex and lots of compounds are present, the Raman bands assignment is difficult. Even more so, if medium and weak bands related with each compound are not evident,

thereby making this task more difficult. As an example of this casuistry, in the Figure 1A different Raman bands obtained from gypsum plasters of the Igueldo Lighthouse are presented. The signals at 981 cm^{-1} and 1006 cm^{-1} (shoulder in $1000\text{--}1010\text{ cm}^{-1}$ region) correspond to syngenite [$\text{K}_2\text{Ca}(\text{SO}_4)_2 \cdot \text{H}_2\text{O}$], the band at 1001 cm^{-1} belongs to glauberite [$\text{CaNa}_2(\text{SO}_4)_2$], the bands at 989 cm^{-1} and 1016 cm^{-1} (shoulder in $1010\text{--}1030\text{ cm}^{-1}$ region) correspond to those of polyhalite [$\text{K}_2\text{Ca}_2\text{Mg}(\text{SO}_4)_4 \cdot 2\text{H}_2\text{O}$] and the 1008 cm^{-1} peak to the main band of gypsum ($\text{CaSO}_4 \cdot 2\text{H}_2\text{O}$). Finally, the bands at 1013 cm^{-1} (shoulder in $1010\text{--}1030\text{ cm}^{-1}$ region), 1048 cm^{-1} and 1067 cm^{-1} are clearly related with the bands of humberstonite [$\text{K}_3\text{Na}_7\text{Mg}_2(\text{SO}_4)_6(\text{NO}_3)_2 \cdot 6\text{H}_2\text{O}$]. Analysing the whole spectrum shown in Figure 1A, the secondary bands of these mineral phases can also be ascertained.⁴ As has been described in the literature, marine aerosols carry airborne particulate matter from sulfates and nitrates. Nitrate particles can be formed following a reaction between marine aerosol sea salts and NO_x gases (NO_2 , N_2O_5 , ClONO_2 etc.) emitted into the atmosphere (e.g. road traffic source etc.). HNO_3 formed after the inclusion of $\text{NO}_{2(g)}$ in rainwater or humidity is reported to be the most important cause of the nitrate particles formation. These particles can react with building materials giving rise to different types of nitrate salts. An example of this is the presence of KNO_3 and NaNO_3 identified by Raman spectroscopy in the sandstone from La Galea Fortress (see Figure 1B). The bands at 1067 cm^{-1} and 724 cm^{-1} belong to nitratine (NaNO_3), while niter (KNO_3) was identified thanks to the presence of its main band at 1048 cm^{-1} and its secondary bands at 712 cm^{-1} , 1344 cm^{-1} and 1358 cm^{-1} . In this spectrum (Figure 1B) thenardite (Na_2SO_4 , main band at 992 cm^{-1} and secondary bands at 451 cm^{-1} , 467 cm^{-1} , 620 cm^{-1} , 630 cm^{-1} , 644 cm^{-1} , 1100 cm^{-1} , 1130 cm^{-1} and 1151 cm^{-1}) was also detected. Apart from this compound, a band at 985 cm^{-1} was also observed, belonging to the main band of epsomite ($\text{MgSO}_4 \cdot 7\text{H}_2\text{O}$). Marine aerosol can carry magnesium

sulfates with different hydration degrees. These sulfates can be deposited on the surface of the building materials as airborne particulate matter.^{2,10,11}

In other cases (see Figure 1C), thenardite (Na_2SO_4) can be observed together with the presence of calcite (CaCO_3 , main band at 1086 cm^{-1} , together with secondary bands at 712 cm^{-1} and 280 cm^{-1}). In Figure 1D, mascagnite [$(\text{NH}_4)_2\text{SO}_4$, the main Raman band at 975 cm^{-1}] was identified. Apart from this sulfate, peaks at 152 cm^{-1} , 280 cm^{-1} , 712 cm^{-1} and 1086 cm^{-1} belonging to calcite (CaCO_3) and 465 cm^{-1} belonging to quartz (SiO_2) were also detected. Mascagnite could be present in the material as airborne particulate matter present in the material following a dry deposition. The deposited ammonium sulfate can penetrate, dissolve and migrate to suffer a recrystallisation process in the inner parts of the material (sandstone) promoting loss of material during time.

In order to extract more information about the decaying compounds and the original composition of the materials, additional elemental analyses based on XRF were carried out. In the Figure 2, an exhaustive XRF analysis on the sandstone from La Galea Fortress is presented. In this case single point and imaging analyses were performed. As can be seen in the accumulated spectrum (see Figure 2 top-centre) of the imaging analysis (21.4 mm height \times 25.9 mm width, $13,803$ pixels) the presence of Al, Si, S, Cl, K, Ca, Ti, V, Mn, Fe, Co, Ni, Cu, Zn, Ga, Pb, As, Br, Rb, Sr, Y, Zr, Sn and Ba was detected. According to the semi-quantitative values determined by the software, Si, Al, Cl, K and Fe are present as major elements; S, Ca, Ti and Cu as minor elements; and the rest as trace elements. This observation confirms that this kind of sandstone has a considerable proportion of calcite. It is important to highlight that sometimes the bremsstrahlung continuum in the spectrum using a Rh tube can contribute to decrease the limit of detection for elements appearing at energies between 7 keV and 18 keV . To increase the limit of detection, lower electron acceleration voltages or filters can be used. An example regarding the

use of filters can be observed in Figure 2 top-right. In this case, due to the use of a $630\text{ }\mu\text{m}$ aluminium filter, the K-lines of Zn and As, elements present in trace levels in the sandstone can be observed more clearly when compared with the measurements without the filter.

Apart from single point analysis, XRF imaging helps us to observe different chemical tendencies along the sandstone. As can be observed in the Al–Si–K map (see Figure 2), pink areas representing the coincident Al–Si distribution are observable. Moreover, in some areas Si is also related with K (light blue areas) suggesting that some of the aluminosilicates in the sandstone could be present as potassium aluminosilicates. In this elemental map, dark blue areas are also highly distributed, representing the α -quartz presence, which is a major component in the sandstone. According to the Cl and Br maps (see Figure 2), these two elements are almost homogeneously distributed on the sandstone, confirming the deposition of these salts coming from the marine aerosol. In the Ca–Sr distribution map (see Figure 2) green areas are observable, representing the combined presence of Ca (yellow) and Sr (light blue). Calcium carbonate could contain Sr in its structure, thus it is not surprising to find a correlation between the distributions of both elements. This observation confirms the presence of calcite in this kind of stone, previously detected by Raman spectroscopy. However, in the same Ca–Sr distribution map, certain hot spots of Ca (yellow) and Sr (light blue) are observable. It is well-known that Sr is highly emitted by marine aerosol, thus Sr hot spots can be related with depositions of this element emitted by the marine aerosol.

In addition to chloride salts, marine aerosol also carries sulfate salts [e.g. arcanite or $\text{K}_2(\text{SO}_4)_2$]. Looking at the S–K map (see Figure 2), the distribution of both elements is coincident in certain areas (orange coloured regions), suggesting a possible deposition of arcanite or a possible chemical transformation of calcite present in the sandstone due to the SO_2 coming from the atmosphere. Finally, in the Ca–S distribution map background, pink areas can

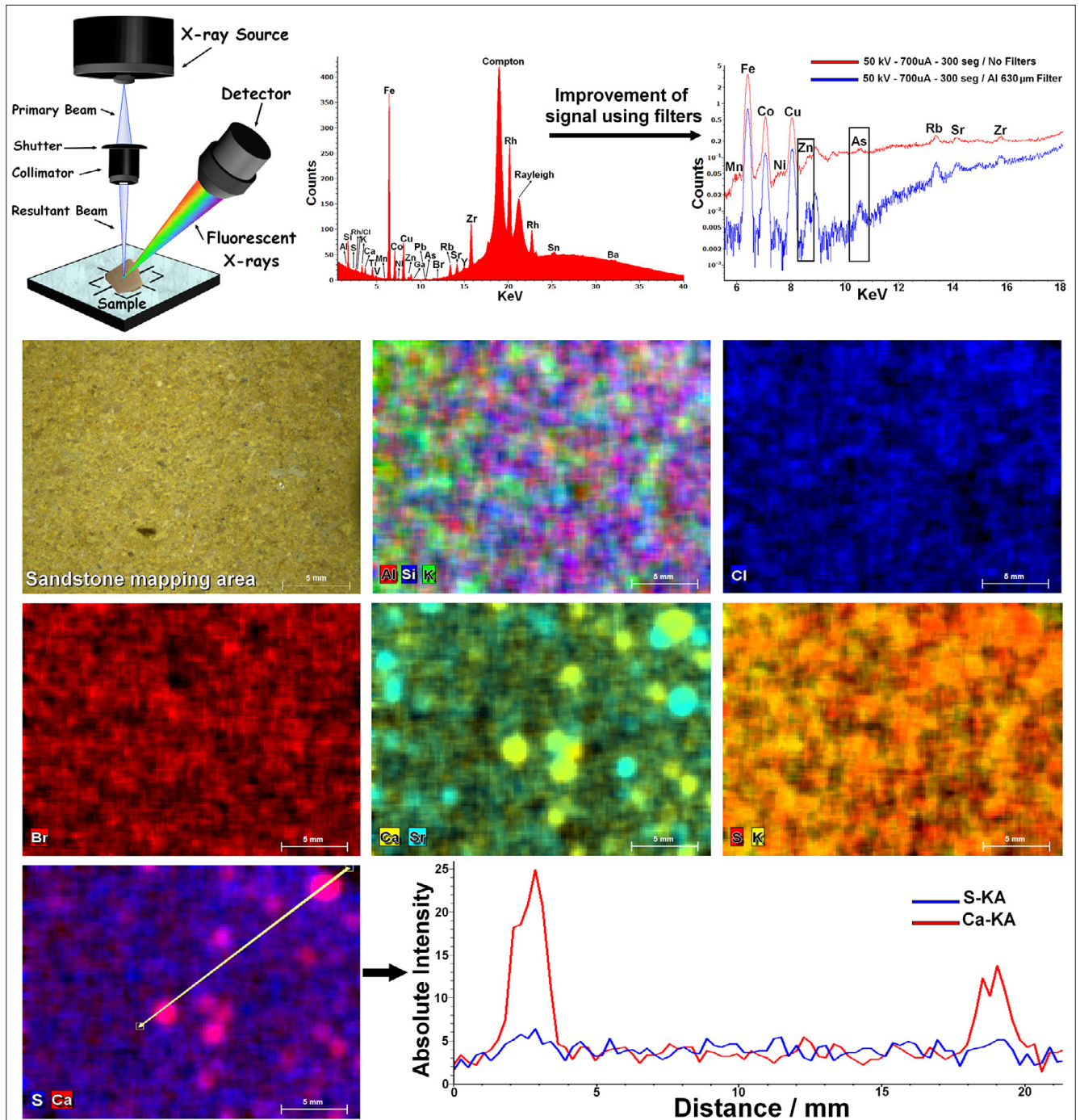


Figure 2. Energy dispersive XRF spectrometer set up illustrating the measurement of a sandstone fragment from La Galea Fortress (top-left), the obtained XRF accumulated spectrum from the XRF imaging analysis (top-centre), spectral results obtained from the XRF single point analysis without (red) and with (blue) a 630 µm Al filter (top-right), Al–Si–K, Cl, Br, Ca–Sr, S–K, S–Ca distribution maps obtained from the XRF imaging analysis (see also the visible image of the mapped sandstone area) of the sandstone and a line scan (bottom-right) showing the variations of the Ca and S K-lines absolute XRF intensity (counts) in the line drawn in the S–Ca distribution map.

be observed. This coincidence in the distribution could point to a transformation of the calcite present in the sandstone into calcium sulfate due to the SO_2 coming from the atmosphere. On the contrary, the pink hotspots could suggest possible

calcium sulfate depositions. Calcite particles can be emitted to the atmosphere due to the erosion of rocks. This carbonate compound can react in the atmosphere with the hydrated SO_2 acid gas (H_2SO_4) to give rise to calcium sulfate. This sulfate

can suffer a subsequent deposition in the building materials following a dry deposition process. The higher signal input (absolute intensity in counts) of Ca and S in the hot spots can be observed in the line scan performed (see Figure 2 bottom-right).

Concluding remarks

In this study, it was possible to characterise different deterioration processes caused mainly by the influence of marine aerosols (wet and dry depositions), infiltration waters, salts migrations, atmospheric acid gases impact (wet and dry depositions) etc., due to the combined use of Raman spectroscopy and ED-XRF. The high amount of sulfates and nitrates present in these atmospheres coming from the marine aerosol itself or from acid gases (SO₂ and NO_x) emitted by urban–industrial sources can modify the original composition of these materials.

These results highlight the importance of the use of such analytical tools to detect the decay compounds and the original composition of the different materials from historical buildings close to the sea, which is fundamental in order to be able to explain the reactions that take place on them. This methodology can assist in the design of recovery actions and in the development of preventive conservation strategies for historical buildings.

Acknowledgements

This work has been funded by the Spanish Ministry of Economy and Competitiveness (MINECO) through the project DISILICA-1930 (ref. BIA2014-59124-P) and the Regional Development Fund (FEDER). H. Morillas is grateful to the University of the Basque Country (UPV/EHU) and mainly to the action UFI 11-26 Global Change and Heritage, who funded his pre-doctoral fellowship.

References

1. H. Morillas, I. Marcaida, M. Maguregui, J.A. Carrero and J.M. Madariaga, "The influence of rainwater composition on the conservation state of cementitious building materials", *Sci. Total Environ.* **542**, 716–727 (2016). doi: <http://dx.doi.org/10.1016/j.scitotenv.2015.10.041>
2. H. Morillas, M. Maguregui, C. García-Florentino, I. Marcaida and J.M. Madariaga, "Study of particulate matter from Primary/Secondary Marine Aerosol and anthropogenic sources collected by a self-made passive sampler for the evaluation of the dry deposition impact on Built Heritage", *Sci. Total Environ.* **550**, 285–296 (2016). doi: <http://dx.doi.org/10.1016/j.scitotenv.2016.01.080>
3. H. Morillas, M. Maguregui, C. García-Florentino, J.A. Carrero, I. Salcedo and J.M. Madariaga, "The cauliflower-like black crusts on sandstones: A natural passive sampler to evaluate the surrounding environmental pollution", *Environ. Res.* **147**, 218–232 (2016). doi: <http://dx.doi.org/10.1016/j.envres.2016.02.015>
4. H. Morillas, M. Maguregui, C. Paris, L. Bellot-Gurlet, P. Colomban and J.M. Madariaga, "The role of marine aerosol in the formation of (double) sulfate/nitrate salts in plasters", *Microchem. J.* **123**, 148–157 (2015). doi: <http://dx.doi.org/10.1016/j.microc.2015.06.004>
5. H. Morillas, M. Maguregui, O. Gómez-Laserna, J. Trebolazabala and J.M. Madariaga, "Characterisation and diagnosis of the conservation state of cementitious materials exposed to the open air in XIX century lighthouses located on the coast of the Basque Country: The case of Igueldo lighthouse, San Sebastian, North of Spain", *J. Raman Spectrosc.* **43**, 1630–1636 (2012). doi: <http://dx.doi.org/10.1002/jrs.4130>
6. H. Morillas, M. Maguregui, O. Gómez-Laserna, J. Trebolazabala and J.M. Madariaga, "Could marine aerosol contribute to deteriorate building materials from interior areas of lighthouses? An answer from the analytical chemistry point of view", *J. Raman Spectrosc.* **44**, 1700–1710 (2013). doi: <http://dx.doi.org/10.1002/jrs.4396>
7. H. Morillas, M. Maguregui, J. Trebolazabala and J.M. Madariaga, "Nature and origin of white efflorescence on bricks, artificial stones, and joint mortars of modern houses evaluated by portable Raman spectroscopy and laboratory analyses", *Spectrochim. Acta A.* **136**, 1195–1203 (2015). doi: <http://dx.doi.org/10.1016/j.saa.2014.10.006>
8. H. Morillas, M. Maguregui, I. Marcaida, J. Trebolazabala, I. Salcedo and J.M. Madariaga, "Characterization of the main colonizer and biogenic pigments present in the red biofilm from La Galea Fortress sandstone by means of microscopic observations and Raman imaging", *Microchem. J.* **121**, 48–55 (2015). doi: <http://dx.doi.org/10.1016/j.microc.2015.02.005>
9. M. Hoyos, S. Sanchez-Moral, E. Sanz-Rubio and J.C. Canaveras, "Alteration causes and processes in the stone material from the pavement in Baelo Claudia archeological site, Cadiz/Spain", *Mater. Construcc.* **49**, 5–18 (1999). doi: <http://dx.doi.org/10.3989/mc.1999.v49.i255.438>
10. L.-Y. Zhao, Y.-H. Zhang, Z.-F. Wei, H. Cheng and X.-H. Li, "Magnesium sulfate aerosols studied by FTIR spectroscopy: hygroscopic properties, supersaturated structures, and implications for seawater aerosols", *J. Phys. Chem. A.* **110**, 951–958 (2006). doi: <http://dx.doi.org/10.1021/jp055291i>
11. S. Maskey, H. Geng, Y.-C. Song, H. Hwang, Y.-J. Yoon, K.-H. Ahn and C.U. Ro, "Attenuated total reflection Fourier transform-infrared imaging techniques", *Environ. Sci. Technol.* **45**, 6275–6282 (2011). doi: <http://dx.doi.org/10.1021/es200936m>



Why the
S8 TIGER?



REASON #13:
Safe sample analysis

SampleCare™ constantly protects important WDXRF system components from contamination, ensuring accurate results and reliable system performance.

www.bruker.com/S8TIGER#13

WDXRF

Synchrotron-based micro Fourier transform infrared mapping to investigate the spatial distribution of amorphous and crystalline calcium carbonate in earthworm-secreted calcium carbonate balls

Mark E. Hodson,^a Liane G. Benning,^{b,c} Gianfelice Cinque,^d Bea Demarchi,^e Mark Frogley,^d Kirsty E.H. Penkman,^e Juan D. Rodriguez-Blanco,^{b,f} Paul F. Schofield,^g Emma A.A. Versteegh^h and Katia Wehbe^d

^aEnvironment Department, University of York, YO10 5DD York, UK. E-mail: mark.hodson@york.ac.uk

^bCohen Laboratories, School of Earth and Environment, University of Leeds, LS2 9JT Leeds, UK

^cGFZ German Research Centre for Geosciences, Helmholtz Centre Potsdam, Telegrafenberg, 14473 Potsdam, Germany

^dBeamline B22, Diamond Light Source, Diamond House, Harwell Science and Innovation Campus, Didcot, Oxfordshire, OX11 0DE, UK

^eBioArCh, Departments of Chemistry and Archaeology, University of York, York, UK

^fNano-Science Center, Department of Chemistry, University of Copenhagen, 2100 Copenhagen, Denmark

^gMineral and Planetary Sciences, Department of Earth Sciences, Natural History Museum, London SW7 5BD, UK

^hSoil Research Centre, Department of Geography and Environmental Science, School of Archaeology, Geography and Environmental Science, University of Reading, Wokingham RG6 6DW, UK

Introduction: earthworms and calcium carbonate

Several species of earthworm, including *Lumbricus terrestris*, often called the lob worm or night crawler, secrete millimetre-scale granules of calcium carbonate (see Figure 1).¹ A number of questions are posed by these granules, not least, the function that they serve (we think they are involved in pH regulation). This article addresses questions about the mineralogical composition of the granules. The granules start off life as a milky fluid, actually a suspension of micron-scale amorphous calcium carbonate, in the rear-most of three pairs of pouches that together form the earthworm's calciferous gland. This gland is located between the 10th and 12th segments

of *L. terrestris*. The milky fluid passes from the rear-most pouch to the fore-most and, in the process, the spherulites aggregate together and largely recrystallise to calcite prior to excretion into the earthworm intestine and from there out into the soil.² The curious thing about the mineralogical composition of the soil-secreted granules is that whilst they are predominantly calcite, a common crystalline form of calcium carbonate, different polymorphs (same chemical composition but the atoms and molecules are arranged differently to give a different mineral form) of calcium carbonate can also be found in the granules—aragonite, vaterite and amorphous calcium carbonate (ACC).^{2,3} We have detected amorphous calcium carbonate in gran-

ules that are several years old, which is rather surprising. If chemists make pure amorphous calcium carbonate in the laboratory using inorganic chemistry, it is extremely unstable, transforming within minutes to the crystalline polymorphs such as calcite. There is experimental evidence that organic molecules can stabilise amorphous calcium carbonate, either by binding to the surface of amorphous calcium carbonate molecular clusters and inhibiting their dissolution and recrystallization, or by binding to Ca²⁺ ions, inhibiting or retarding their interaction with HCO₃⁻ and CO₃.²⁻⁴

In this study we wished to determine whether the ACC in the granules was stabilised by organic molecules. Aside from good old fashioned scientific curi-

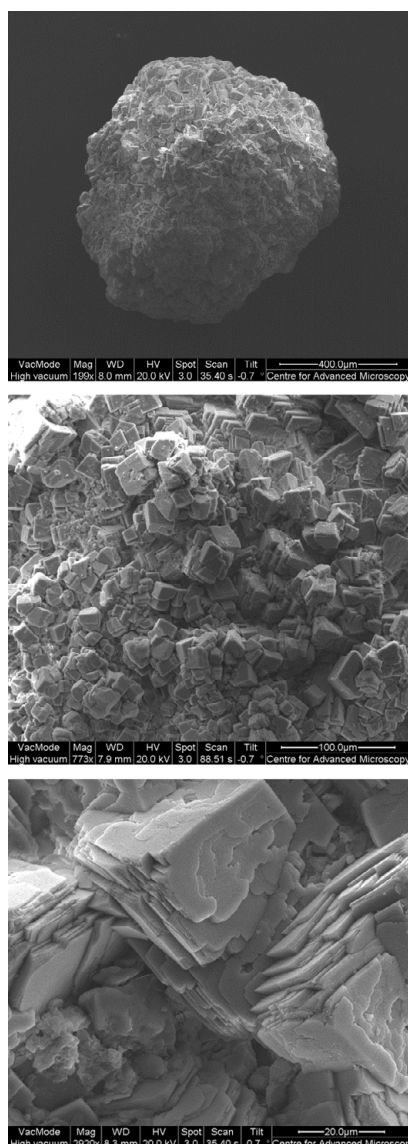


Figure 1. Granules of calcium carbonate secreted by the earthworm *L. terrestris*. Top, scale bar 400 µm; middle, scale bar 100 µm; bottom, scale bar 20 µm.

osity there are potential industrial benefits in understanding the stability of the different forms of calcium carbonate as this material is used in a whole host of industries.

Initially we worked on the bulk composition of the granules using Fourier transform infrared (FT-IR) spectroscopy but then we carried out some spatially resolved analyses with synchrotron-based μ -FT-IR mapping at Beamline B22 (Multimode InfraRed Imaging And Microspectroscopy, MIRIAM) of the Diamond Light Source, in the UK.

The bulk composition of the granules

Our first challenge was to collect some granules. We purchased some *L. terrestris* earthworms from Worms Direct (Drylands, Ulting, Nr Maldon, Essex CM9 6QS, UK). Thanks to fishermen and gardeners there are good commercial supplies of this species of earthworm. We collected soils from a range of different locations around Berkshire, UK, dried the soil and then sieved it to $<250\ \mu\text{m}$. We then moistened the soil and cultivated earthworms in it for 27 days. The earthworms were removed and the soil sieved to $<500\ \mu\text{m}$. This allowed us to collect the granules, that are $\approx 2\ \text{mm}$ in diameter, which had been excreted into the soil. Subsamples of these granules were ground and the powders analysed by FT-IR spectroscopy using an A2-Technology (Danbury, USA) MicroLab portable mid-IR spectrometer fitted with a diamond internal reflection (DATR) capability in order to determine the form of calcium carbonate present and by liquid chromatography for their amino acid content.

Calcium carbonate is easily identified using FT-IR spectroscopy (see Figure 2). Crystalline carbonate phases such as calcite have distinct bands at $\sim 714\ \text{cm}^{-1}$ (ν_4), $\sim 866\ \text{cm}^{-1}$ (ν_2), $\sim 1084\ \text{cm}^{-1}$ (ν_1) and $1420\text{--}1470\ \text{cm}^{-1}$ (ν_3) whilst ACC lacks the distinct vibrational band at $\sim 714\ \text{cm}^{-1}$.

The FT-IR spectra of the bulk granules had differing peak area ratios for both the $\nu_2:\nu_4$ and the $\nu_3:\nu_4$ bands indicating differing ratios of amorphous calcium carbonate (higher ratio) to crystalline calcium carbonate (lower ratio) in the granules. We could not detect bands in the spectra corresponding to organic molecules present within the granules but this could have been due to low concentrations and detection issues.

The liquid chromatography that we carried out on the granules did indicate the presence of a range of amino acids. These may have been present initially as amino acids or proteins, our extraction method breaks proteins up into their amino acid building blocks. When we compared the amino acid content

**Accelerate publication
of your MS review
with EJMS Accounts**



*EJMS Accounts are
published online
within six weeks, and
shortly after in print.*

EJMS Accounts provide concise reviews of active areas of mass spectrometry research. They are normally written by scientists who have strong current interests in the areas. They should be succinct and lucid, they can be polemical and they ought to predict future developments.

*Try out extremely fast
publication for Accounts*

**[www.impublications.com/
landing/6-weeks.html](http://www.impublications.com/landing/6-weeks.html)**

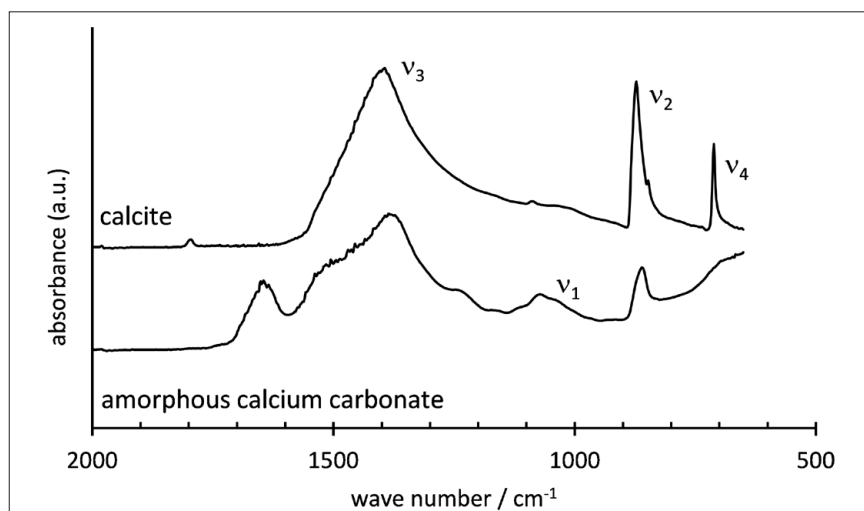


Figure 2. Typical FT-IR spectra of calcite, a crystalline calcium carbonate, and amorphous calcium carbonate.

of the granules to the peak area ratios we saw good correlations between the two for various amino acids such as aspartic acid/asparagine, glutamic acid/glutamine and phenylalanine. Although correlation does not equal causation, this suggests that the proteins

or amino acids might be stabilising the amorphous calcium carbonate. To investigate this further we decided to carry out spatial analysis to see whether the organic molecules were associated with the amorphous calcium carbonate or not.

Spatial analysis of the granules

First, we collected some more earthworm granules. We embedded these granules in EpoFIX (Struers) resin blocks and ground away the resin to expose cross sections through the granules. These samples were analysed at beamline B22 of the Diamond Light Source using a Bruker Vertex 80 V FT-IR instrument connected to a Hyperion 3000 microscope to produce μ -FT-IR maps. Spectra were collected in reflectance mode with a liquid N₂ cooled Mercury-Cadmium-Telluride (MCT) broadband detector, and at a resolution of 4 cm⁻¹ by co-adding between 128 and 1024 scans per point. Both large (*ca* 700 μ m \times 700 μ m, 20–25 μ m aperture, internal globar and synchrotron sources onto a gold mirror and zinc selenide substrate, respectively) and small (*ca* 100 μ m \times 150 μ m, 6 μ m aperture, synchrotron source, gold mirror reference) scale maps were produced of areas of the granule cross sections.

We attempted to map out the distribution of amorphous calcium carbonate

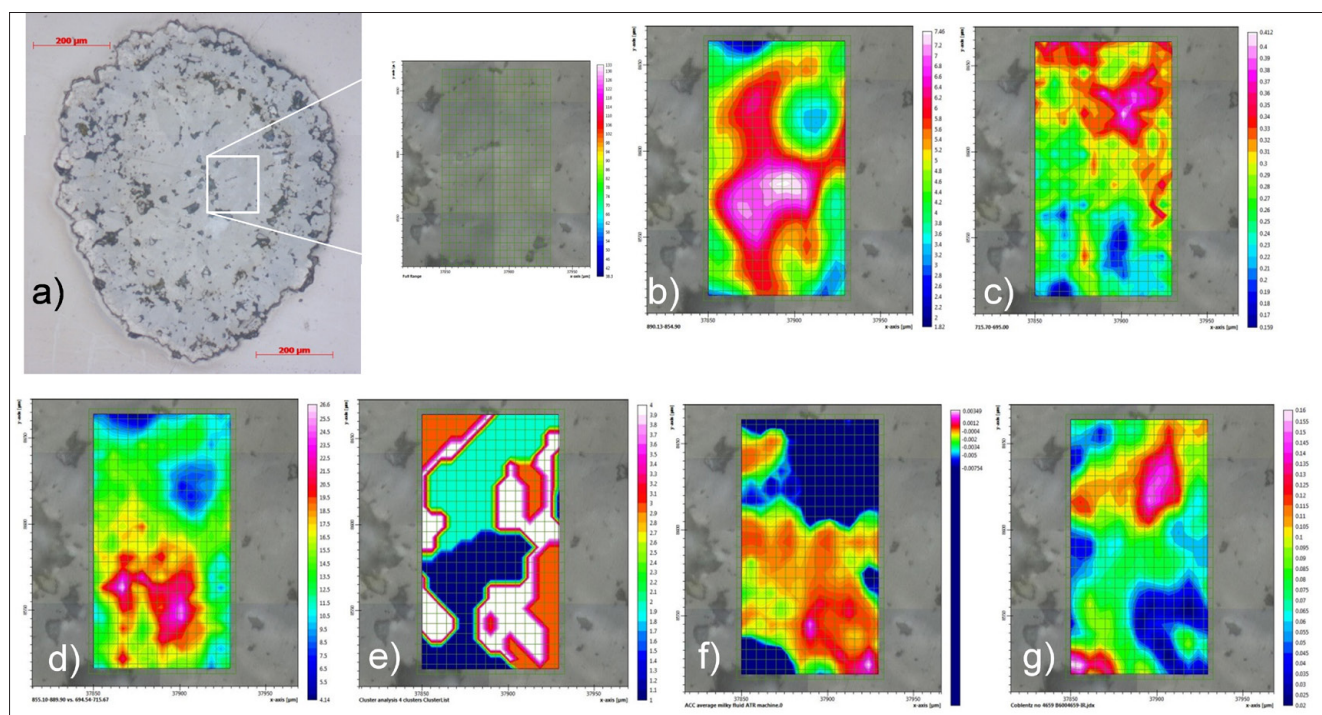


Figure 3. Images and intensity maps from synchrotron-based μ -FT-IR mapping of an earthworm-secreted calcium carbonate granule. Scale bar in a) is 200 μ m. a) Reflected light image of a cross-section through a granule; b) 855–890 cm⁻¹ (v_2), c) 695–716 cm⁻¹ (v_4) and d) $v_2:v_4$ ratio intensity maps suggesting the presence of amorphous calcium carbonate in the lower half of the map and calcite in the upper half; e) cluster analysis maps showing areas of distinctly different FT-IR spectra in the upper and lower halves of the map; f) amorphous calcium carbonate and g) calcite component regression intensity maps suggesting amorphous calcium carbonate in the lower half of the maps and calcite in the upper half. For μ -FTIR intensity maps, red indicates high intensity and blue indicates low intensity. This figure is taken from Hodson *et al.* (2015).⁵

in the granules by processing our data in four independent ways using Opus 7.2 (Bruker) software. In the most direct approach we mapped out the intensity of the FT-IR signal between 855 cm^{-1} and 890 cm^{-1} (for the ν_2 peak) and 695 cm^{-1} and 716 cm^{-1} (for the ν_4 peak) and the ratio of the two. The $\nu_2:\nu_4$ peak ratio should be highest for regions of ACC. Second, we carried out cluster analysis on the second derivative of the $855\text{--}890\text{ cm}^{-1}$ and $695\text{--}716\text{ cm}^{-1}$ regions of the spectra following vector normalisation. Although this method did not allow us to identify amorphous and crystalline calcium carbonate it identified areas with similar FT-IR spectra. Finally, we used standard amorphous calcium carbonate and calcite spectra (see Figure 2) to carry out component regression on our maps, considering the $650\text{--}1200\text{ cm}^{-1}$ range. The resulting intensity maps show how good a fit there is between the standard spectrum (either ACC or calcite) and the spectrum at each point on the FT-IR spectroscopic map. These four independent methods all identified similar areas as being likely to comprise amorphous calcium carbonate (see Figure 3). There was good correspondence between areas with a high $\nu_2:\nu_4$ peak ratio and the areas that showed the best match to the standard amorphous calcium carbonate spectrum. Similarly there was good correspondence between the areas with a low $\nu_2:\nu_4$ peak ratio and the areas that showed the best match to the standard calcite spectrum. Finally, the cluster analysis identified areas with distinct FT-IR spectral characteristics that corresponded to the high and low $\nu_2:\nu_4$ peak areas.

Having identified ACC we had hoped to identify bands related to organic compounds in our spectra as well to see whether there was any relationship between the two. We did not see a peak at 1650 cm^{-1} where the amide I band should occur and unfortunately our spectra had a broad peak in the $1570\text{--}1350\text{ cm}^{-1}$ wavenumber range where we had hoped to see distinct peaks at 1540 cm^{-1} and 1450 cm^{-1} corresponding to the amide II and lipid/amide III bands, respectively. The ν_3 peak of calcite is also present in this range (at

$1420\text{--}1470\text{ cm}^{-1}$). To date we have been unable to deconvolute this mixed component peak. We are now attempting to use another spectroscopic technique—scanning transmission X-ray microscopy—at the Diamond Light Source (Beamline I08), to do the same job using Ca X-ray absorption near edge spectroscopy (XANES) maps to identify the form of calcium carbonate present and CXANES to determine whether any of the carbon present in amorphous calcium carbonate regions is present as organic carbon rather than carbonate.

Acknowledgements

This work was funded by NERC grants NE/F009623/1 and NE/H021914/1A, a White Rose Consortium grant and beamtime at the Diamond light source under grants SM9197 and SM8989. We thank the Leverhulme Trust for financial support to the NEaer laboratory, University of York and Sheila Taylor (University of York) for provision of technical support for amino acid analyses.

References

1. M.G. Canti and T.G. Pearce, "Morphology and dynamics of calcium carbonate granules produced by different earthworm species", *Pedobiol.* **47**, 511–521 (2003). doi: <http://dx.doi.org/10.1078/0031-4056-00221>
2. L. Gago-Duport, M.J.I. Briones, J.B. Rodríguez and B. Covelo, "Amorphous calcium carbonate biomineralization in the earthworm's calciferous gland: Pathways to the formation of crystalline phases", *J. Struct. Biol.* **162**, 422–435 (2008). doi: <http://dx.doi.org/10.1016/j.jsb.2008.02.007>
3. L. Brinza, P.F. Schofield, M.E. Hodson, S. Weller, K. Ignatyev, K. Geraki, P.D. Quinn and J.F.W. Mosselmans, "Combining μ XANES and μ XRD mapping to analyse the heterogeneity in calcium carbonate granules excreted by the earthworm *Lumbricus terrestris*", *J. Synchrotron Rad.* **21**, 235–241 (2014). doi: <http://dx.doi.org/10.1107/S160057751303083X>
4. D.J. Tobler, J.D. Rodríguez-Blanco, K. Dideriksen, K.K. Sand, N. Bovet, L.G. Benning and S.L.S. Stipp, "The effect of aspartic acid and glycine on amorphous calcium carbonate (ACC) structure, stability and crystallization", *Proc. Earth Planet. Sci.* **10**, 143–148 (2014). doi: <http://dx.doi.org/10.1016/j.proeps.2014.08.047>
5. M.E. Hodson, L.G. Benning, B. Demarchi, K. Penkman, J.D. Rodríguez-Blanco, P.F. Schofield and E.A.A. Versteegh, "Amorphous calcium carbonate stability in earthworm-secreted granules: an amino acid and synchrotron FTIR study", *Geochem. Trans.* **16**, 4 (2015). doi: <http://dx.doi.org/10.1186/s12932-015-0019-z>

Why the S8 TIGER?



REASON #17: Speaks your language

The S8 TIGER's TouchControl™ user interface provides free, online language selections that make the WDXRF analysis accessible to over 80% of the world's population.

www.bruker.com/S8TIGER#17

WDXRF

Infrared spectroscopic techniques for the non-invasive and rapid quality control of Chinese traditional medicine Si-Wu-Tang

C.K. Pezzej,^{a,§} M. Watschinger,^{a,§} V.A. Huck-Pezzej,^a C.B.S. Lau,^b Z. Zuo,^c P.C. Leung^b and C.W. Huck^{a,*}

^aInstitute of Analytical Chemistry and Radiochemistry, CCB-Center for Chemistry and Biomedicine, Innrain 80/82, 6020 Innsbruck, Austria. E-mail: Christian.W.Huck@uibk.ac.at

^bInstitute of Chinese Medicine and State Key Laboratory of Phytochemistry and Plant Resources in West China, The Chinese University of Hong Kong, Shatin, New Territories, Hong Kong

^cSchool of Pharmacy, The Chinese University of Hong Kong, Shatin, New Territories, Hong Kong

[§]Contributed equally

Introduction

A fast and non-destructive quality control of Si-Wu-Tang (SWT), one of the most used Traditional Chinese Medicine (TCM) formulae against women's diseases is presented in this article. The authentication method was established using attenuated total reflectance-mid-infrared (ATR-MIR) and near infrared (NIR) spectroscopy in combination with multivariate data analysis (MVA). Measurements were performed applying MIR and NIR bench-top spectrometers. Additionally a laboratory-independent hand-held NIR device was employed enabling on-site characterisation. The spectra were subjected to different data-pretreatments such as multiplicative signal correction (MSC), first and second derivative to remove systematic errors and then evaluated applying a principal component analysis (PCA). A distinction between SWT samples and its adulterants could be achieved with all three devices. Because of its ease of use, and its fast and reliable analysis results, infrared (IR) spectroscopy is becoming increasingly important for the quality control of pharmaceutically relevant herbs.

Traditional Chinese Medicine as a well-established health care system is increasingly gaining popularity worldwide. It has been used in China and other Asian countries for over 5000 years for the prevention and treatment of many different diseases. Compared with Western medicine, TCM uses a holistic and synergistic approach to restore the body's homeostasis.¹ Due to its growing popularity, more and more scientific studies deal with the quality control of such products. Several analytical techniques like high performance liquid chromatography, gas chromatography or capillary chromatography for the analysis of bioactive constituents have been reported in the literature.^{2,3} All of them are destructive, time and chemical consuming. Therefore the aim of this study was to establish a simple, rapid and non-invasive authentication method for one of the most popular TCM formulae, Si Wu Tang (SWT), and its raw herbs using MIR and NIR spectroscopy.

Si Wu Tang

SWT is used for the treatment of women's diseases such as the ease of menstrual discomfort, dysmenorrhea and other

oestrogen caused inconveniences.⁴ It is widely used in Asia, especially China, but as shown in a recent study it can also be integrated into Western medicine as an alternative therapy.⁵

It is composed of four herbs, i.e. Radix Paeoniae Alba, Rhizoma Chuanxiong, Radix Angelicae Sinensis and Radix Rehmanniae Preparata.⁶ The main secondary metabolites present in these four herbs are phenolics, phthalides, alkaloids, terpene glycosides and iridoid glycosides. The identified bioactive components reported in the literature are gallic acid, paeoniflorin and paeonol from Paeonia;⁷⁻⁹ ferulic acid, Z-ligustilide and senkyunolide A from Angelica;^{10,11} ferulic acid, Z-ligustilide, ligustrazine, butylphthalide and senkyunolide A from Chuanxiong;^{11,12,3} and catalpol from Rehmannia.¹³ For paeoniflorin, ferulic acid and Z-Ligustilide, antimutagenic, antioxidative, antiallergic and anti-inflammatory activities have been reported.¹⁴⁻¹⁶

Materials and methods

Materials

All samples were provided by the School of Pharmacy and Institute of Chinese

Medicine of The Chinese University of Hong Kong (CUHK).

Three samples of SWT manufactured by the CUHK according to the Chinese Pharmacopeia 2010⁶ with slight modifications and four commercially available SWT were obtained. Furthermore, three samples of each single herb extract manufactured by the CUHK and one commercially available sample of each single herb extract of which SWT is composed (Radix Paeoniae Alba, Rhizoma Chuanxiong, Radix Angelicae Sinensis, Radix Rehmanniae Preparata) were received. The sample set also included five non-SWT samples. These are the commercially available Danshen Gegen composed of *Salvia miltiorrhiza* and *Puerariae lobata* as well as Huang Qin consisting of *Scutellaria baicalensis* Georgi. Three non-SWT samples were manufactured by the CUHK, i.e. ELP (Epimedii Herba, Ligustri Lucidi Fructus and Psoraleae Fructus), Penta Herb Formula and Danshen Gegen. All samples provided by the CUHK are considered to be representative analysis samples. For homogenisation all samples were ground in a mortar. The samples were stored together with a silica gel sachet in order to avoid water absorption.

ATR-MIR spectroscopy

ATR-MIR spectra were collected with a PerkinElmer Spectrum 100 ATR-IR spectrometer (PerkinElmer, Waltham, USA) in combination with a Spectrum software version 6.3.1.0134 (PerkinElmer, Waltham, USA). The recorded wavenumber range was 4000–650 cm^{-1} at a spectral resolution of 4 cm^{-1} . Every sample was divided into three subsamples and 16 scans per subsample were taken. Measurements were undertaken at 22°C.

NIR spectroscopy

Spectra were obtained with a Büchi NIRFlex N-500 FT-NIR spectrometer (Büchi, Flawil, Switzerland) using NIR Ware 1.4.3010 (Büchi, Flawil, Switzerland). A Büchi solids device equipped with a vial add-on was utilised for diffuse reflectance measurements. Every sample was measured in triplicate accumulating 16 scans for each

spectrum. Recorded wavenumbers were 10,000–4000 cm^{-1} with a resolution of 8 cm^{-1} .

In order to perform laboratory-independent measurements, a MicroPhazir (Thermo Scientific, USA) was used, which was operated between 6266 cm^{-1} and 4173 cm^{-1} at a resolution of 21 cm^{-1} . Each sample was measured six times and 10 scans per sample were accumulated.

NIR measurements were performed at 22°C.

Multivariate data analysis

Multivariate data analysis was performed with The Unscrambler 10.3 software package (Camo, Oslo, Norway) employing PCA with the non-linear iterative partial least squares algorithm (NIPALS). PCA models for the quality control of SWT and its raw herbs were developed for all three devices (for MIR and NIR benchtop spectrometers, and for the mobile NIR device). Prior to further data-pretreatments, spectra were transformed to $\log 1/R$ ($R = \% \text{ reflectance}$) except for the data from the hand-held device which were already obtained in absorbance. All spectral data were baseline corrected and normalised and an average spectrum of each sample was

generated. Different pretreatments such as first and second derivative Savitzky–Golay or standard normal variate (SNV) were applied to the spectra. For the derivatives the ideal number of smoothing points was evaluated and is given below in brackets, e.g. first derivative (9). All models were calculated applying full cross validation.

Results

Benchtop MIR spectroscopy

An averaged ATR-MIR spectrum of all analysed SWT samples is presented in Figure 1. The following main bands were observed: 3305 cm^{-1} (O–H stretching of water and carbohydrates), 2977 cm^{-1} (C–H antisymmetric stretching), 2886 cm^{-1} (C–H symmetric stretching), 1621 cm^{-1} (C=O stretching, conjugated; C=C stretching) and 1011 cm^{-1} (C–O, C–C stretching, mainly of carbohydrates). Band assignments are according to Pretsch *et al.*¹⁷

Distinction of SWT and non-SWT

As data-pretreatment, SNV and a first derivative (11) were employed. The inter-spectral variance is optimally described with two principal components (PCs). Figure 2a shows the 2D score plot, indicating appropriate clus-

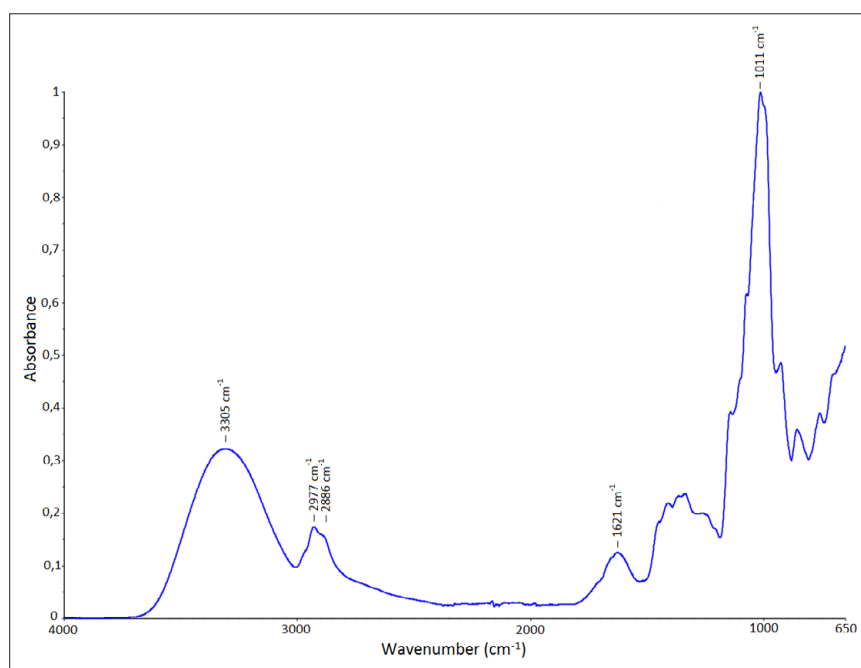


Figure 1. Averaged ATR-MIR spectrum of SWT samples.

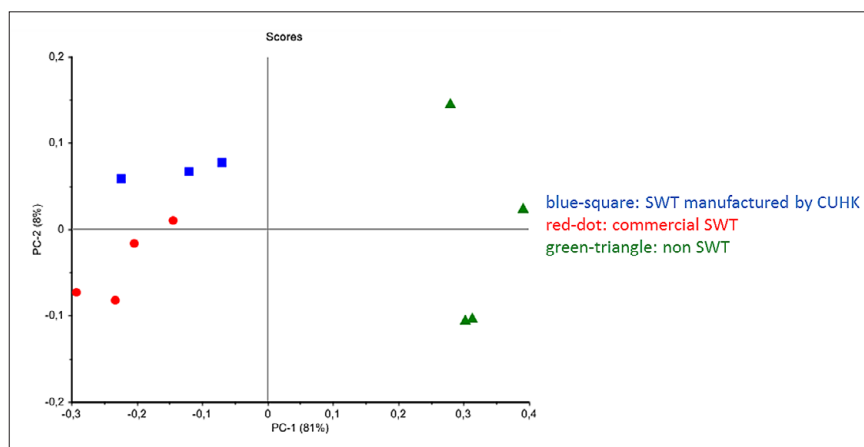


Figure 2a. PCA score plot obtained with the benchtop ATR-MIR spectrometer.

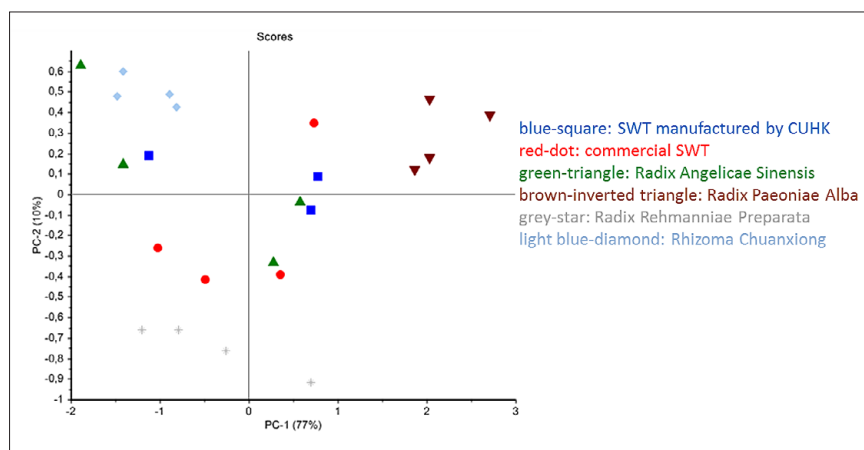


Figure 2b. PCA score plot obtained with the benchtop ATR-MIR spectrometer.

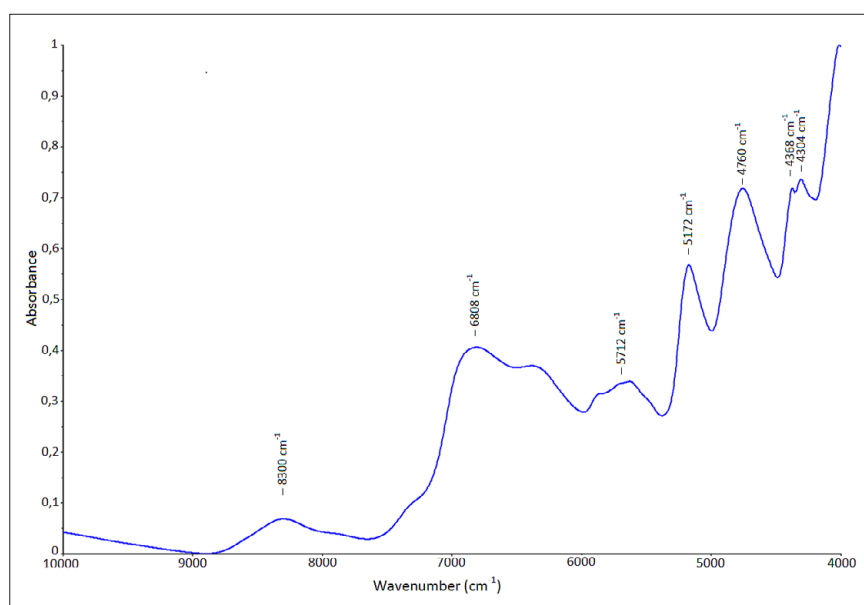


Figure 3. Averaged NIR spectrum of SWT samples recorded with the benchtop NIR spectrometer.

tering of the samples. The SWT samples can be clearly separated from the non-SWT samples. Furthermore, a distinction between SWT samples manufactured by the CUHK and commercially available SWT samples is evident.

SWT with respect to its raw herbs

Successful clustering of SWT samples and its raw herb extracts was realised applying the first two PCs (Figure 2b). Only Radix Angelicae Sinensis samples are distributed widely. The SWT samples are centrally arranged relative to its raw herb clusters indicating that the herbal remedy is composed of Radix Paeoniae Alba, Rhizoma Chuanxiong, Radix Angelicae Sinensis and Radix Rehmanniae Preparata.

Benchtop NIR spectroscopy

A typical NIR spectrum recorded with the benchtop NIR device is shown in Figure 3. The characteristic bands were assigned as: 8300 cm^{-1} (C–H stretching second overtone), 6808 cm^{-1} (O–H first overtone, phenols, H_2O), 5712 cm^{-1} (C–H stretching first overtone), 5172 cm^{-1} (O–H stretching and deformation combination, H_2O , polysaccharides), 4760 cm^{-1} (C–H stretching and deformation combination, O–H stretching and C–O deformation combination, carbohydrates), 4368 cm^{-1} (C–H stretching and C–H deformation combination) and 4304 cm^{-1} (C–H stretching and C–H deformation combination). The vibrational bands were assigned according to Workman *et al.*¹⁸ and Chalmers *et al.*¹⁹

Distinction of SWT and non-SWT

The principal component analysis in Figure 4a is based on spectra that have been subjected to a second derivative (11). The spectral variance is described with four latent variables of which the first and fourth variables have been found to correlate best with the investigated problem. A successful discrimination between SWT and non-SWT samples can be achieved and also the SWT manufactured by CUHK can clearly be distinguished from the SWT samples which are commercially available.

Why the S8 TIGER?

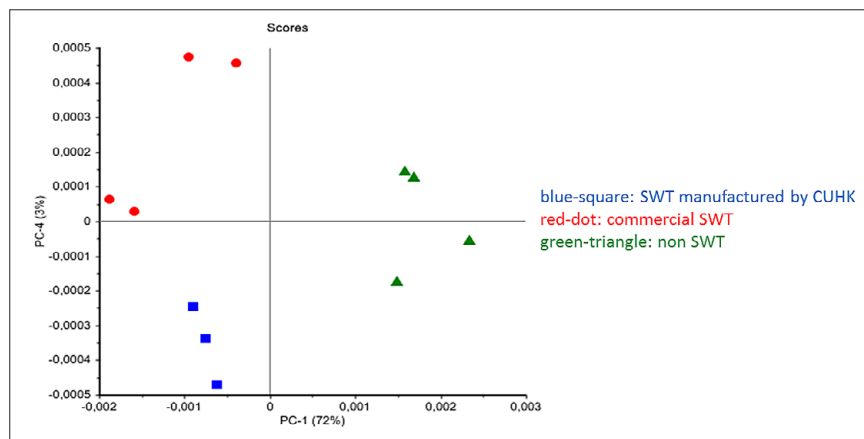


Figure 4a. PCA score plot obtained with the benchtop NIR spectrometer.

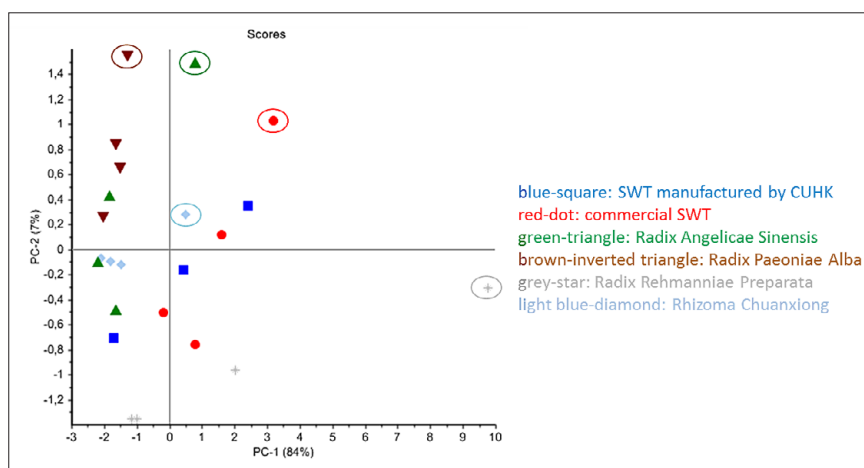


Figure 4b. PCA score plot obtained with the benchtop NIR spectrometer.

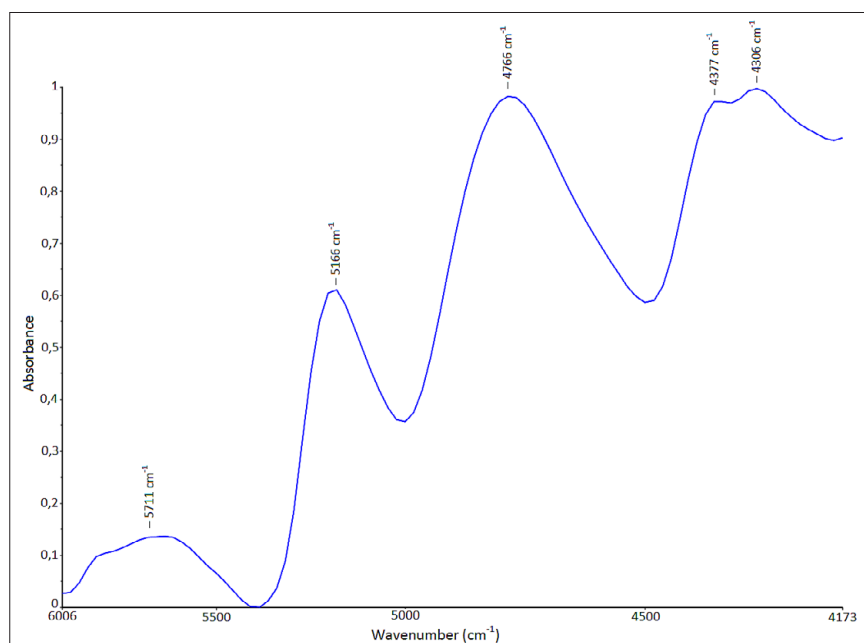


Figure 5. Averaged NIR spectrum of SWT samples recorded with the mobile NIR spectrometer.



REASON #23: Quality components

Core technologies, including X-ray generator, goniometer, X-ray detector and analyzer crystals, have been developed by Bruker, specifically for use in the S8 TIGER WDXRF.

www.bruker.com/S8TIGER#23

WDXRF

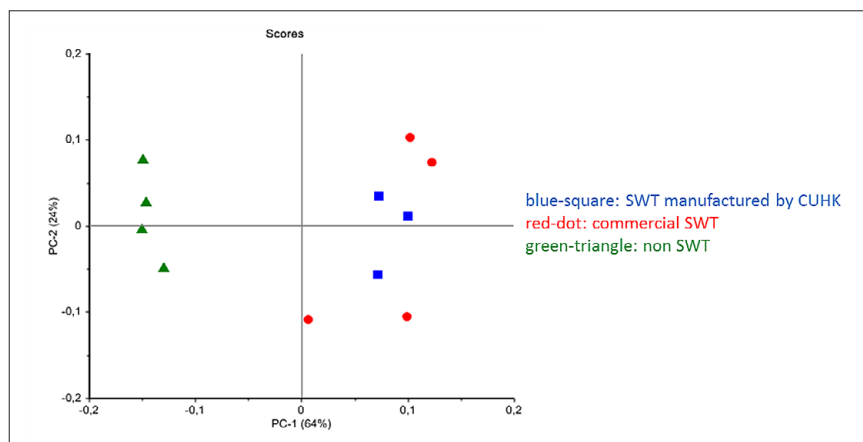


Figure 6a. PCA score plot obtained with the mobile NIR spectrometer.

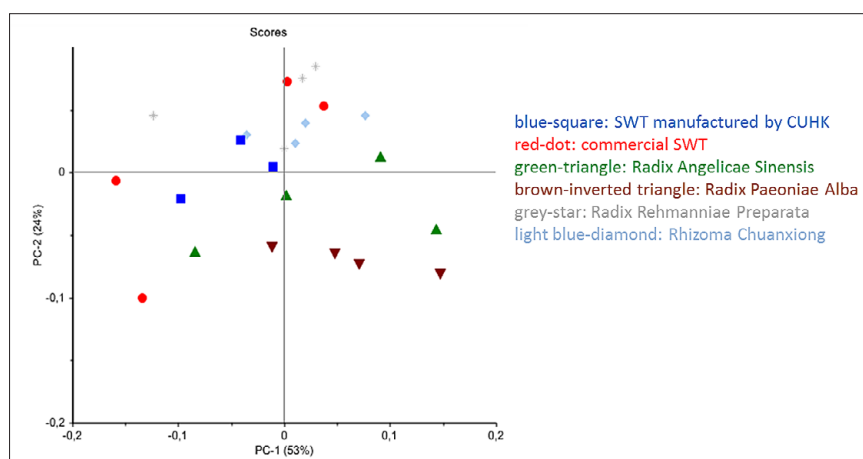


Figure 6b. PCA score plot obtained with the mobile NIR spectrometer.

SWT with respect to its raw herbs

The best results of the PCA were achieved with a SNV pretreatment. The score plot in Figure 4b shows that for the raw herb samples, always one batch out of the four batches of each single herb extract is outside its related cluster. These samples (marked with a circle) of Radix Paeoniae Alba, Rhizoma Chuanxiong, Radix Angelicae Sinensis and Radix Rehmanniae Preparata are all commercially available and were purchased from the same manufacturer. The other samples of raw herbs were manufactured by the CUHK. Regarding the SWT cluster it could be observed that the commercially available SWT (marked with a circle) which is not correctly assigned was again purchased from the same manufacturer as the commercially available raw herbs. Thus these samples can

clearly be distinguished from samples manufactured by the CUHK.

Mobile NIR spectroscopy

A typical NIR spectrum recorded with the mobile NIR device is shown in Figure 5. The following main bands were assigned: 5711 cm^{-1} (C–H stretching first overtone), 5166 cm^{-1} (O–H stretching and deformation combination, H_2O , polysaccharides), 4766 cm^{-1} (C–H stretching and deformation combination, O–H stretching and C–O deformation combination, carbohydrates), 4377 cm^{-1} (C–H stretching and C–H deformation combination) and 4306 cm^{-1} (C–H stretching and C–H deformation combination). Band assignment was done according to Workman *et al.*¹⁸ and Chalmers *et al.*¹⁹

Distinction of SWT and non-SWT

Because of the promising results of the benchtop NIR spectrometer, a hand-held NIR spectrometer was used to enable on-site quality control of the products. As data-pretreatment, SNV and a first derivative (7) were used. Applying the first two PCs, the SWT samples can definitely be differentiated from the non-SWT samples (Figure 6a). Compared to the benchtop NIR-derived score plot, SWT manufactured by the CUHK cannot be distinguished from the commercially available SWT.

SWT with respect to its raw herbs

The evaluation of different data-pretreatments revealed that SNV in combination with a first derivative was most suitable for the given application. The 2D score plot in Figure 6b displays that the SWT samples as well as the raw herbs are arranged in a wider cluster in comparison to the benchtop NIR device.

Discussion

From the data presented it can be concluded that vibrational infrared spectroscopy is highly suitable for a quick and non-invasive quality control of SWT and its raw herbs. All three devices, i.e. the MIR and NIR benchtop spectrometers and the mobile NIR device displayed satisfactory performances. The SWT samples could be clearly distinguished from adulterations and a successful clustering of the raw herb extracts was achieved. Best results were produced by the benchtop NIR device for which samples manufactured by the CUHK could be clearly distinguished from commercially available samples. The performance of the hand-held NIR device is, despite its limited spectral range and lower resolution, still precise enough for a fast identification enabling laboratory-independent quality control of TCM products. The results of this study are considered as an important step towards reliable on-site measurements of herbal remedies. Mobile devices are becoming increasingly important in qualitative and quantitative analysis,

supporting the demands of laboratory-independent methods.

Acknowledgements

Special thanks to the Federal Ministry of Science, Research and Economy (Vienna, Austria), project "Novel analytical tools for the quality assessment of Chinese herbs with metabolic, immune related neuromodulatory effects" (BMFW – 402.000/0017-WF/V/6/2016).

References

1. T. Efferth, P.C.H. Li, V.S.B. Konkimalla and B. Kaina, "From traditional Chinese medicine to rational cancer therapy", *Trends Mol. Med.* **13**, 353–361 (2007). doi: <http://dx.doi.org/10.1016/j.molmed.2007.07.001>
2. P.-S. Xie and A.Y. Leung, "Understanding the traditional aspect of Chinese medicine in order to achieve meaningful quality control of Chinese materia medica", *J. Chromatogr. A* **1216**, 1933–1940 (2009). doi: <http://dx.doi.org/10.1016/j.chroma.2008.08.045>
3. H. Zhang, P. Shen and Y. Cheng, "Identification and determination of the major constituents in traditional Chinese medicine Si-Wu-Tang by HPLC coupled with DAD and ESI-MS", *J. Pharm. Biomed. Anal.* **34**, 705–713 (2004). doi: [http://dx.doi.org/10.1016/S0731-7085\(03\)00650-2](http://dx.doi.org/10.1016/S0731-7085(03)00650-2)
4. Q. Hao, J. Wang, J. Niu, P. Zhao and Y. Cui, *Acta Chin. Med. Pharm.* **36**, 10–15 (2008).
5. J.-F. Cheng, Z.-Y. Lu, Y.-C. Su, L.-C. Chiang and R.-Y. Wang, "A traditional Chinese herbal medicine used to treat dysmenorrhoea among Taiwanese women", *J. Clin. Nurs.* **17**, 2588–2595 (2008). doi: <http://dx.doi.org/10.1111/j.1365-2702.2008.02382.x>
6. The State Pharmacopoeia Commission of P.R. China, *Pharmacopoeia of the People's Republic of China*. China Medical Science and Technology Press (2010).
7. Y.-X. Sheng, L. Li, Q. Wang, H.-Z. Guo and D.-A. Guo, "Simultaneous determination of gallic acid, albiflorin, paeoniflorin, ferulic acid and benzoic acid in Si-Wu decoction by high-performance liquid chromatography DAD method", *J. Pharm. Biomed. Anal.* **37**, 805–810 (2005). doi: <http://dx.doi.org/10.1016/j.jpba.2004.11.002>
8. F.L. Hsu, C.W. Lai and J.T. Cheng, "Antihyperglycemic effects of Paeoniflorin and 8-debenzoylpaeoniflorin, glucosides from the root of *Paeonia lactiflora*", *Planta Med.* **63**, 323–325 (1997). doi: <http://dx.doi.org/10.1055/s-2006-957692>
9. C.H. Lau, C.M. Chan, Y.W. Chan, K.M. Lau, T.W. Lau, F.C. Lam, W.T. Law, C.T. Che, P.C. Leung, K.P. Fung, Y.Y. Ho and C.B.S. Lau, "Pharmacological investigations of the anti-diabetic effect of Cortex Moutan and its active component paeonol", *Phytomedicine* **14**, 778–784 (2007). doi: <http://dx.doi.org/10.1016/j.phymed.2007.01.007>
10. F. Cui, L. Feng and J. Hu, "Pharmacological investigations of the anti-diabetic effect of Cortex Moutan and its active component paeonol", *Drug Dev. Ind. Pharm.* **32**, 747–755 (2006). doi: <http://dx.doi.org/10.1080/03639040500529101>
11. W.-Y. Huang and S.-J. Sheu, "Separation and identification of the organic acids in Angelicae Radix and Ligustici Rhizoma by HPLC and CE", *J. Sep. Sci.* **29**, 2616–2624 (2006). doi: <http://dx.doi.org/10.1002/jssc.200600136>
12. S.S.-K. Chan, T.-Y. Cheng and G. Lin, "Pharmacological investigations of the anti-diabetic effect of Cortex Moutan and its active component paeonol", *J. Ethnopharmacol.* **111**, 677–680 (2007). doi: <http://dx.doi.org/10.1016/j.jep.2006.12.018>
13. Y.-Y. Tian, L.-J. An, L. Jiang, Y.-L. Duan, J. Chen and B. Jiang, "Catalpol protects dopaminergic neurons from LPS-induced neurotoxicity in mesencephalic neuron-glia cultures", *Life Sci.* **80**, 193–199 (2006). doi: <http://dx.doi.org/10.1016/j.lfs.2006.09.010>
14. S. Ou and K.-C. Kwok, "Ferulic acid: pharmaceutical functions, preparation and applications in foods", *J. Sci. Food Agric.* **84**, 1261–1269 (2004). doi: <http://dx.doi.org/10.1002/jsfa.1873>
15. Y.-Q. Zheng, W. Wei, L. Zhu and J.-X. Liu, "Ferulic acid: pharmaceutical functions, preparation and applications in foods", *Inflamm. Res.* **56**, 182–188 (2007). doi: <http://dx.doi.org/10.1007/s00011-006-6002-5>
16. J. Du, Y. Yu, Y. Ke, C. Wang, L. Zhu and Z.M. Qian, "Ligustilide attenuates pain behavior induced by acetic acid or formalin", *J. Ethnopharmacol.* **112**, 211–214 (2007). doi: <http://dx.doi.org/10.1016/j.jep.2007.02.007>
17. E. Pretsch, P. Bühlmann and M. Badertscher, *Spektroskopische Daten zur Strukturklärung organischer Verbindungen*. Springer (2010). doi: <http://dx.doi.org/10.1007/978-3-540-76866-1>
18. J. Workman and L. Weyer, *Practical Guide to Interpretive Near-Infrared Spectroscopy*. CRC Press (2008).
19. J.M. Chalmers and P.R. Griffiths, *Handbook of Vibrational Spectroscopy*. John Wiley & Sons (2002). doi: <http://dx.doi.org/10.1002/0470027320>



Starna

THE SCIENCE OF COMPLIANCE



The World Leader in UV,
Visible and NIR Certified
Reference Materials
ISO/IEC 17025 Calibration
NIST Traceable
ISO Guide 34 Reference
Material Producer
Lifetime Guarantee
Fast Recalibration Service

sales@starna.com
www.starna.com
+44(0) 20 8501 5550



There are standards—and there is *the* standard

Kim H. Esbensen^a and Claas Wagner^{b,*}

^aKHE Consulting, www.kheconsult.com

^bSampling Consultant—Specialist in Feed, Food and Fuel QA/QC. E-mail: cw@wagnerconsultants.com

This series of columns has come to a natural half-way stage, at which it is worth reflecting a little. The basic principles for sampling of heterogeneous stationary lots, materials and systems have been covered—it is time start thinking of sampling from moving lots, dynamic systems and processes. But first: the Theory of Sampling (TOS) is proclaimed to be the only complete theory with which to address all the world's many types of materials with a view of guaranteeing representative samples, and the column makes an effort, hopefully appreciated and easy to follow, to explain all the elements and their relationships in this endeavour. However, many standards, guidelines and norm-giving documents (CEN, ISO) already exist, which include elements of prescriptions for "proper sampling", such as have been agreed upon by numerous task forces, committees etc. as being fit-for-purpose within the relevant scientific, trade and technological contexts addressed. There have been many such fits and starts towards a recommended sampling practice, but always in a partial sense only, indeed *none* cover the full breadth of all that is necessary to master representative sampling (with two spectacular exceptions: the iron ore and cement industry sectors). With so many partial recommendations available, when not in compliance with respect to TOS, there are objective, serious contradictions. *Que faire?*

The situation

The publication of DS 3077¹ represented the world's first standard dedicated exclusively to representative sampling. Hardly any other standard is in full compliance with the appropriate TOS requirements laid out here, although *partial* elements can be found in many places, e.g. see the bibliography in DS 3077.¹ Two notable exceptions exist, however, the cement and the iron ore industries, which have been well serviced with excellent standards in this context for many years.

Non-compliance issues regarding such standards, guidelines, good practices as well as regulatory and legal requirements must be handled with insight and patience. Where found not to comply with TOS' stipulations, it will be necessary to start a process of revision or updating of the relevant standards or norm-giving documents—which may be a lengthy process, and one that requires quite some logistical and organisational drive. While this is taking place, or when dictated by documented sampling variances that are too high (a key issue in quality control and assurance, QC/QA), it is always an option to

employ more stringent quality criteria from a TOS-based approach than what is specified in today's imperfect standards. As there are serious economic and societal consequences of non-representative sampling, simply staying with "following the book" is never a sound strategy, scientifically as well as regarding the economic outcome of decisions which will then in reality be based on inferior, non-representative data. DS 3077 has the overall objective of establishing a comprehensive motivation and competence for taking the stand relying *only* on fully TOS-compliant sampling procedures and equipment irrespective of the theoretical, practical, technological, industrial or societal context under the law. No standard is a legal document on its own and is therefore not legally binding; all trade agreements ruled by international standards are based on a set of voluntary agreements. To the extent that international law on the subjects treated in standards dealing with sampling aspects has been adopted, this law must be adhered to. International law implemented in national laws also takes precedence to non-legal documents in case of conflict.

Be this as it may, there are very many advantages in not being complacent with the fact that sampling issues are mentioned in the existing body of relevant standards and norm-giving documents. Mentioning is not enough, only the principles guaranteeing representativity matter. A directed effort has been in place for some five years, involving a systematic critique of selected standards, specifically with respect to the full set of sampling errors outlined in TOS. Two examples of this work are presented below, which suffice to show how one should approach any part of a standard etc. that purports to recommend proper sampling procedures and equipment etc.

Analysis of sampling standards for solid biofuels

Assessment of all sampling procedures from CEN standards for sampling solid biomass (CEN/TS 14778 part 1 and part 2)^{2,3} has shown that most of the recommended procedures do not lead to a fully satisfactory result, a representative sample. Correct delineation and extraction of many standardised methods as well as depicted, and thus

SAMPLING COLUMN

recommended, tools and equipment are *not* ensured. While for grab and shovelling methods, correct delineation and extraction is hardly ever possible, other recommended sampling methods lack sufficient specification regarding application conditions, which invariably increases the potential for incorrect sampling error effects. Table 1 gives an overview of the evaluation results with respect to potential *incorrect sampling errors* (ISE) caused by the methods stated, recommended or allowed in the standard for primary sampling CEN/TS 14778.^{2,3} ISE comprise the three so-called bias-generating errors: Increment Delimitation/Delineation Error (IDE), Increment Extraction Error (IEE) and Increment Preparation Error (IPE), all concerning sampling equipment and sampling procedures. The full assessment of these sampling standards can be found in Wagner & Esbensen.⁴

Insufficient specifications and the existence of incorrect sampling errors must under all circumstances be eliminated in sampling standards as the result will unavoidably be an inconstant *sampling bias*, always and for ever out of control; it is not possible to make any bias correction regarding the sampling bias, DS 3077¹ and Esbensen & Wagner.⁵ Incorrect sampling methods, room for personal interpretation and the vertical standardisation approach of CEN specifying different procedures for each mate-

rial group makes sampling a complicated issue with a highly uncertain and varying validity. Any procedure and standard that has not eradicated all such potential sampling bias elements, as illustrated above, does not comply with TOS' stringent and demands for sampling correctness. The result is always a biased sampling procedure—which is always unacceptable. The full assessment of CEN/TS 14778 has been published, but so far no reaction or response has been forthcoming.⁴

Analysis of grain sampling guide

The "Home Grown Cereals Authority" (HGCA) is a division of the "Agriculture and Horticulture Development Board" based in the UK, which is mainly responsible for research and knowledge transfer in the cereal and oilseed sector. In 2013 the HGCA published a guide on grain sampling to define key requirements for effective grain sampling at various process locations from harvest to storage until departure and arrival of the grain.⁶ Besides physical extraction of a grain "sample", focus is also on monitoring moisture, temperature, pests and moulds, especially mycotoxins. The described sampling practices therefore must have an obligation to contribute to ensure procedures that reliably are able to assess harvested grain quality, to protect this quality level throughout the

storage phase as well as to determine the quality level after storage (before transportation to buyer) and upon arrival at the buyer. For various commodities the latter two aspects (differences in quality level at departure vs quality level at arrival) have in the past caused major law cases, often due to inappropriate or inadequate sampling procedures. Besides these kinds of discrepancies which cause serious economic disputes, extraction of representative grain samples is also crucial with regard to impurity detection (e.g. GMO quantification, toxins), as regulated by international standards (e.g. ISO 24276:2006⁷). Table 2 gives an overview of the evaluation results for the HGCA⁶ with respect to potential TOS-incorrect sampling errors. The full assessment can be found in *TOS forum*.⁸

This assessment shows that most of its recommended sampling procedures and equipment (for both primary sampling and sub-sampling) do *not* lead to a representative sample. The guide's sampling procedures have a high error potential for incorrect sample delineation and extraction, which unavoidably will lead to a significantly detrimental, or even fatal sampling bias.¹ Most of the guide's recommended sampling equipment, when rated with TOS criteria, reveal major incorrect sampling errors (ISE), vastly jeopardising grain control validity. It is noteworthy that the body responsible for the HGCA guide undertook a

Table 1. Assessment of incorrect sampling errors of CEN/TS 14778.

	IDE	IEE	IPE
Three-dimensional lot	Sampling from stationary lot		
	High error potential	High error potential	Medium error potential
One-dimensional lot	Conveyer belt		
	High error potential Low error potential	Medium error potential	Medium error potential
Automatic sampling	High error potential Low error potential	High error potential	Medium error potential
	Falling source stream		
Manual sampling	High error potential	High error potential	Medium error potential
Automatic sampling	High error potential Low error potential	High error potential Low error potential	Low error potential

SAMPLING COLUMN

Table 2. Assessment of incorrect sampling errors of HGCA sampling guide.

Process location (HGCA)	IDE	IEE	IPE
Sampling at harvest			
Method 1: Sampling before cleaning/drying—Sampling of trailer as it is tipped into store	High error potential	High error potential	Low error potential
Method 2: Sampling after conditioning—Sampling from the cleaner/dryer outlet	High error potential	High error potential	Low error potential
Sampling in store			
Sampling spear (3–5 apertures)	High error potential	Medium error potential	Low error potential
		Low error potential	
Sampling at outloading			
Sampling from loading bucket	High error potential	High error potential	Low error potential
Automatic bucket sampler	High error potential	High error potential	Low error potential
Sampling from spout loading Jug/Bucket Interrupter plate	High error potential	High error potential	Low error potential
	Medium error potential	Medium error potential	
Sampling from grain heap	High error potential	Medium error potential	Low error potential
	Medium error potential	Low error potential	
Sampling at commercial intakes			
Manual or automatic sampling spear	High error potential	Medium error potential	Low error potential
	Medium error potential	Low error potential	

careful response to the above critique, which was published in *TOS forum* (see box section).⁹

It is in the interest of the science of sampling to bring this kind of discussion to the attention of everybody interested in representative sampling. While the present authors of the critique of the HGCA⁶ do not agree with most of the “reasons for lowering the standard w.r.t. representativity” in the rebuttal (see above), both science and industry *will* benefit from the clearly stated argumentation vs the original critique. It is, as always, up to the reader to form his/her own conclusions based on the evidence presented *pro et con*.

Sampling for GMO risk assessment

Currently an EFSA-funded project is a.o. engaged in a similar critique of all standards and norm-giving documents governing sampling for GMO risk assessment. The project reports will,

after approval by EFSA, be available on the appropriate homepages within the EFSA portal.

Examples of too glib recommendations

For want of space, we end this column by showing a few examples “from undisclosed standards” of a few “recommended” sampling procedures/equipment, which would not under any circumstances find acceptance under the systematics of the Theory of Sampling, TOS (Figures 1–5).

The reader is invited to try to determine which sampling error(s) are compromised in each specific example. It is not relevant to refer to the specific standards from which the examples originate; they are shown here in complete anonymity with the sole purpose of illustrating that sampling is not a game in which anything goes... More seriously, they are examples of what can happen when committees

are guided by a regimen of consensus where truly *anything goes*, as long as it is unanimously voted and agreed on... Pierre Gy often used to deliver a wry comment on this state of affairs in his lectures and courses: “With this approach a committee could vote that Newton’s second law no longer applies”. The few examples are a vivid illustration to this dictum—very many “recommended” sampling procedures and equipment are nothing but a showcase of not having invested the necessary effort to investigate the basics of TOS principles. But, there is always room for improvement.

Summary

There is no need for unnecessary confrontations, but there is a need for absolute clarity with respect to the responsibility carried by international (and national) standardisation authorities. There is no excuse for recommending non-compliant sampling procedures

A critical assessment of the HGCA grain sampling guide

Claas Wagner^{a,*} and Kim. H. Esbensen^{b,a}

^aACABS Research Group, Aalborg University, campus Esbjerg (AAUE), Denmark

^bGeological Survey of Denmark and Greenland, Copenhagen, Denmark. E-mail: claas.wagner@googlemail.com

HGCA's grain sampling guide is assessed with respect to the principles for representative sampling as set forward in the Theory of Sampling (TOS). Sampling correctness, which requires the elimination of all Incorrect Sampling Errors (ISE), constitutes the only guarantee for valid, representative grain quality control; presence of ISEs causes a varying, uncontrollable sampling bias that cannot be corrected for. Contrary to a first superficial observation ("grain is grain"), many different species and varieties, as well as differences caused by soil types, availability of local nutrients, make "grain" a significantly heterogeneous commodity, which requires special attention when sampled at various process locations (from harvesting, storage until commercial intake). The present appraisal shows that most of the respected HGCA grain guide's recommendations do not comply with TOS principles of sampling correctness. The suggested sampling procedures constitute major error potentials, which strongly compromise sample representativity.

Introduction

The "Home Grown Cereals Authority (HGCA) Grain Sampling Guide" (HGCA) is a document issued by the UK grain industry and the Home Office, which is mainly responsible for the oilseed sector. As a part of the AHDB and HGCA and processor representatives with an aim to "deliver the industry through independence and investment".¹ In 2011, HGCA published a guide on grain sampling at various process locations, from harvest until departure of the grain.² Besides physical properties of the grain "sample", focus is also on moisture, temperature, and especially mycotoxins. The sampling practices must therefore be such that they reliably are able to protect the vested grain quality, to protect the level throughout the storage period, as to determine quality level (before transportation to buy arrival at the buyer. For various reasons, the latter two aspects (quality level at departure vs quality level at arrival) have in the past caused several cases, not seldom due to inadequate sampling procedures, such discrepancies causing economic disputes, extraction of representative grain samples is also crucial with respect to impurity detection (e.g. GMO quarantine toxins), as regulated by international standards (e.g. ISO 24276:2006).³

The following critical assessment of HGCA's grain sampling guide serves to

evaluate whether

and offloading processes.

In the current appraisal Table 1 shows the basic sampling methods of the guide opposed with the understanding of these

representative sample, and aggregate sampling in the grain chain". The agreements with the definitions in TOS, are alarmingly narrow as

basic sampling theory that the term used in the HGCA is a property of the property of the number stated in the case the precision), but has accuracy. Accuracy is ensured by sampling core-generating Sampling Errors")

Furthermore, a process also ensures that all in the lot probability implying must have sample. For practical sampling the above must also hold for the operational unit, the "increment". The FSP condition is missing entirely with HGCA.

Dear TOS Forum,
 Thank you for publishing the recent critique of the HGCA Grain Sampling Guide, which raises some interesting and thought-provoking issues for anyone involved with practical on-farm sampling.
 We thought it might be helpful for your readers to explain HGCA's approach as set out in the Guide, which is focused on providing growers with a practical and cost-effective means of sampling—particularly at very busy times such as during harvest.
 The methods outlined were developed to be suitable for growers in real, on-farm situations where time is constrained and resources are often limited.
 The Guide was drawn up in close conjunction with the UK arable industry to reduce errors as far as practically possible and to provide growers with a realistic and basic level of information about the physical properties of their grain.
 This information will help growers understand whether their grain meets contractual specifications on attributes such as moisture, protein levels, specific weight and Hagberg Falling Number.
 The Guide's working assumption is that these attributes will follow a normal distribution, so the protocol is sufficient to give a basic, but useful, level of information about the farmer's crop.
 In addition, grain coming from a single field can be regarded as reasonably homogeneous because it is a single variety that has largely received the same agronomic management and has been exposed to the same soil and weather conditions.
 This context is somewhat different to the Theory of Sampling principles to which you compare the HGCA Guide. These principles are very rigorous and are more suitable for finding contaminants present at a low inclusion rate, and is not necessarily what is required on-farm.
 All the information within the guide was written to adhere to:
 • BS EN ISO 24333:2009 Cereals and cereal products – sampling
 • BS EN ISO 542:1990 Oilseeds – sampling
 Growers and the UK grain industry will continue to work towards the common objective of providing an improved understanding of grain quality which meets both contractual and due diligence requirements.
 As the UK industry moves forward, HGCA will ensure its Grain Sampling Guide is reviewed regularly and we will continue to look at how issues such as those raised in your article can be better reflected in our on-farm advice.
 Yours sincerely
 Dr Dhan Bhandari (HGCA) and Dr Ken Wildey (Technology for Growth)

SAMPLING COLUMN

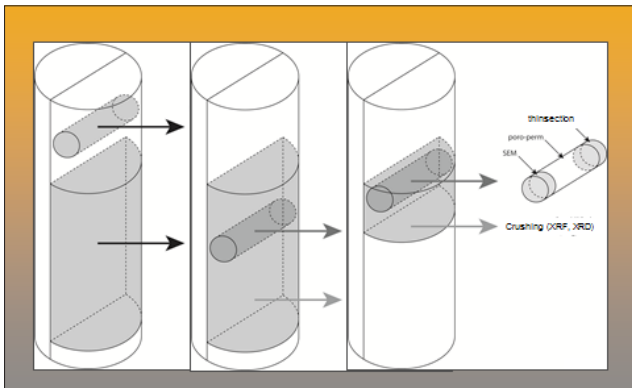


Figure 1. From the geological realm. Sub-sampling a drill core (vertical) with an aim of providing analytical samples for diverse analytical modalities [SEM, porosity and permeability measurements (poro-perm), thin section (petrological microscopy), XRF, XRD]. Although a serious attempt at creating a standardised sub-sampling scheme (left: original recommendation), there is clearly room for improvements as seen in the centre and right-most evolutions towards the smallest coeval sample volume, i.e. the maximum possible joint sample support. There are plenty of arguments from geologists to the tune: “the rocks in the drill core are pretty well homogenous, so some 15–30 cm vertical separation does not matter much... ” or endless variations on this theme, which, however, completely misses the point: There is no need deliberately to create significant IDE and IEE errors in the sampling process (which is tantamount deliberately to create the fatal sampling bias). Also, homogenous materials do not exist in the real world, especially not in the poly-phase heterogeneous worlds of rocks... While there may very well be rocks of particular low vertical heterogeneity that need drilling (e.g. limestone/chalk oil reservoir rocks), setting of a standardised sub-sampling scheme for all reservoir rocks based on this scenario can only lead to significant sampling bias. Allowing for this is not the role of a standard.

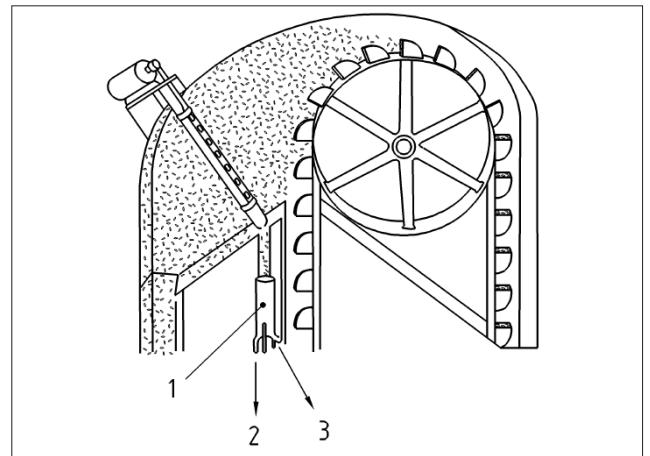


Figure 2. A particularly ill-conceived recommendation of a “grain stream sampler”. When this example was used as a basis for an exam question in a PhD course on “Representative Sampling, TOS” a student wrote: “The mind boggles!”.

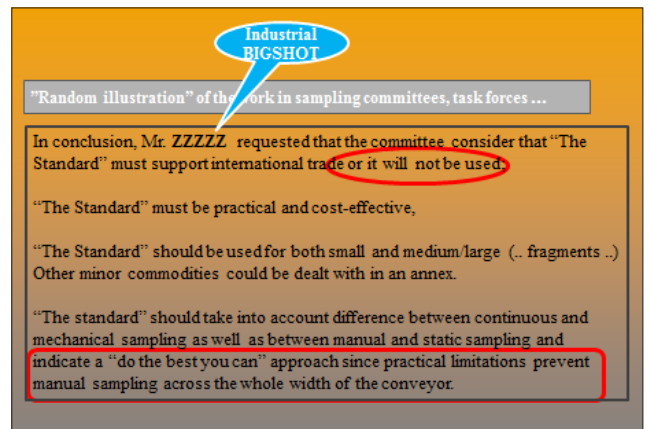


Figure 4. A potpourri of verbatim quotes from discussions in sampling committees and fora. The mind boggles at the lack of respect for representativity, while logistics, practicality and economics would appear to be the only drivers. The effect of letting such proxies dictate sampling procedures, operations and equipment alone was discussed thoroughly, and dismissed, by Esbensen *et al.*^{10,11} and Minkinen *et al.*¹²

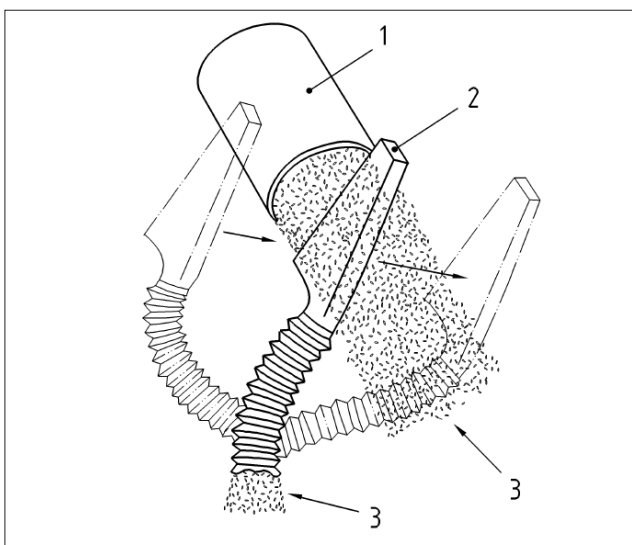


Figure 3. A recommended sampler with a much better chance of being approved by TOS—although the conditions under which this equipment is to operate are totally missing, making it open to several fundamental uncertainties.



Figure 5. Using a cylindrical coring tool for cheese sampling (left) does not allow a representative sample of the highly irregularly distributed components of a mature blue cheese. Only the two right-hand approaches will pass muster for TOS.

SAMPLING COLUMN

and equipment; the result can only be inferior sampling and inferior, indeed compromised, decision making. A chain is only as strong as its weakest link. TOS-compliance is the *missing link* in very many standards etc. There is only one remedy—get involved, get TOS literate!

There are plenty of relevant courses, lectures, consulting companies, experts on the subject matter of representative sampling, all contributing and doing a remarkable job in the last 15 years (for some up to 40 years), but none will receive specific identification here. All the reader needs is a willingness to start looking for the singular operative characteristic: representativeness—as in representative sampling and the Theory of Sampling (TOS).

Que faire?

Start here: DS 3077!¹

References

1. DS 3077, "DS 3077. Representative sampling—Horizontal Standard". Danish Standards (2013). www.ds.dk
2. CEN/TS 14778-1:2005 *Solid Biofuels. Sampling. Part 1: Methods for Sampling*. British Standards Institution, London, UK (2006).
3. CEN/TS 14778-2:2005 *Solid Biofuels. Sampling. Methods for Sampling Particulate Material Transported in Lorries*. British Standards Institution, London, UK (2006).
4. C. Wagner and K.H. Esbensen, "A critical review of sampling standards for solid biofuels – Missing contributions from the Theory of Sampling (TOS)", *Renew. Sust. Energ. Rev.* **16**, 504–517 (2012). doi: <http://dx.doi.org/10.1016/j.rser.2011.08.016>
5. K.H. Esbensen and C. Wagner, "Theory of Sampling (TOS) versus measurement uncertainty (MU)—a call for integration", *Trends Anal. Chem. (TrAC)*, **57**, 93–106 (2014). doi: <http://dx.doi.org/10.1016/j.trac.2014.02.007>
6. *HGCA Grain Sampling Guide*. HGCA Publications, Warwickshire (2013). http://www.hgca.com/media/248889/grain_sampling_guide_2013.pdf (accessed February 2014).
7. ISO 24276:2006 *Foodstuffs—Methods of Analysis for the Detection of Genetically Modified Organisms and Derived Products—General Requirements and Definition*. International Organization for Standardization (ISO), Geneva, Switzerland (2006).
8. C. Wagner and K. Esbensen, "A critical assessment of the HGCA grain sampling guide", *TOS forum* **2**, 16–21 (2014). doi: <http://dx.doi.org/10.1255/tosf.18>
9. D. Bhandari and K. Wildey, "Letter in response to 'A critical assessment of the HGCA grain sampling guide' published *TOS forum* Issue 2", *TOS forum*, **4**, 4–4 (2015). doi: <http://dx.doi.org/10.1255/tosf.36>
10. K.H. Esbensen, C. Paoletti and P. Minkinen, "Representative sampling of large kernel lots – I. Theory of Sampling and variographic analysis", *Trends Anal. Chem. (TrAC)* **32**, 154–165 (2012). doi: <http://dx.doi.org/10.1016/j.trac.2011.09.008>
11. K.H. Esbensen, C. Paoletti and P. Minkinen, "Representative sampling of large kernel lots – III. General Considerations on sampling heterogeneous foods", *Trends Anal. Chem. (TrAC)* **32**, 179–184 (2012). doi: <http://dx.doi.org/10.1016/j.trac.2011.12.002>
12. P. Minkinen, K.H. Esbensen and C. Paoletti, "Representative sampling of large kernel lots – II. Application to soybean sampling for GMO control", *Trends Anal. Chem. (TrAC)* **32**, 166–178 (2012). doi: <http://dx.doi.org/10.1016/j.trac.2011.12.001>

Exceptionally Fast Scanning Spectroscopy

Coming soon to the Jenway range

Model 7200 introduces a new fast scanning visible diode array spectrophotometer to the Jenway range. With a large colour touchscreen interface this instrument is simple to set up and navigate and live spectrum and kinetics runs can be viewed easily. This spectrophotometer has measurement modes for photometrics, concentration, optical density, quantitation, spectrum scanning and kinetics.

This spectrophotometer will be available to order soon. Visit Jenway.com for more details.

- Scanning diode array technology
- Touchscreen navigation
- Small footprint and lightweight
- Fast scan speed
- French language option
- Results saving to USB memory stick
- Extensive range of accessories available



JENWAY



www.jenway.com

A Bibby Scientific Brand

Analytica report 2016

Ian Michael

I am going to continue with the same layout from the Pittcon Report in the last issue, which I think works well. This report, from Analytica, held in Munich, Germany, from 10 to 13 May is inevitably much shorter than that from Pittcon. Many new products at Pittcon were introduced to Europe at Analytica, but we have not covered them again. However, there was plenty that was new and interesting.

Agilent introduced a new version of their 5100 ICP-OES, the 5110. This has an integrated valve system that increases productivity, running a sample every 20s. There is also a new version of the ICP Expert software, and existing users can upgrade to this and to the other improvements. Applied Spectra's J200 is a tandem laser ablation-laser-induced breakdown spectroscopy instrument. LIBS is performed on the emitted light from a laser ablation plasma whilst ablated particles are transferred to an ICP-MS instrument. This enables analysis of organic and lighter elements, elemental mapping, the normalisation of the ICP-MS signal with plasma emission and the simultaneous measurement of major/trace elements and isotopes.

Shimadzu introduced the AIM-9000 Infrared Microscope System, a fully automated system aimed at failure analysis. It provides automation of all steps in failure analysis and micro-sample evaluation: observation, definition of measurement spots, measurement and identification. The AIM-9000 is compatible with Shimadzu's IRAffinity-1S and IRTracer-100 FT-IR spectrometers. With the latter instrument, it can reach a signal-to-noise ratio of 30,000:1 (transmission, MCT detector, 50 μm aperture, 8 cm^{-1} resolution, 2min scan). The Adulterant Screen software from PerkinElmer automates FT-IR and NIR spectrometers that can confirm authenticity and perform nutritional analysis in a single step. It performs rapid, targeted and non-targeted screening for several types of adulterants and can be implemented quickly without the need for lengthy calibration. Spectrolytic introduced the static(s)FTIR which does not contain any moving parts and is very robust. It has a spectral resolution of 6 cm^{-1} , wavelength range from 7 μm to 14 μm and can measure at a modulation frequency of 50Hz.

A fully automated sample preparation system for clinical mass spectrometry came from Shimadzu. The CLAM-2000 (Clinical Laboratory Automated sample preparation Module) automates the pre-treatment of liquid blood or other biological systems prior to LC-MS analysis. It is intended for those handling blood samples in pharmaceutical departments, medical departments or biological analysis laboratories dealing with issues of variability in analytical results or infection risk. It processes samples in parallel and provides full automation through to LC-MS analysis.

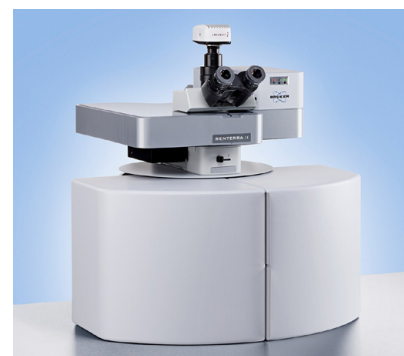
Bruker's Senterra II is an easy-to-use, confocal, multi-laser Raman imaging microscope with various acquisition modes to optimise speed or spatial resolution. The Raman engine has been redesigned to improve spectral resolution and perfor-



The AIM-9000 Infrared Microscope System from Shimadzu



Shimadzu's clinical MS automated sample preparation system, the CLAM-2000



The Senterra II confocal, multi-laser Raman imaging microscope from Bruker

ANALYTICA 2016

mance, and imaging and wavelength calibration is provided by SURE_CAL technology. Components such as motorised lasers, gratings, filters and apertures allow fully automated parameter setting. WITec introduced a new entry-level micro-Raman system, the alpha300 access as well as a thorough revision of the established alpha300 series. The alpha300 access is available at a lower price and, as with all WITec instruments, can be upgraded and expanded.

Sarspec are a Portuguese company new to me. They have a range of miniature spectrometers and were releasing the FAbS, a new compact double-beam spectrophotometer which can also be used as a fluorimeter. Full spectra can be collected in up to 1 ms per spectrum over the full wavelength range and the optical resolution is 0.6 nm. Various sampling options can be achieved via easy fibre optic coupling. They were also showing the S1S fibre-optic spectrometer that can collect 10,000 full spectra per second and has an optical resolution better than 0.2 nm; this will be available early in 2017. Mettler Toledo's UV/VIS Excellence range includes four models including life science and μ L models. The UV7 complies with EU and US Pharmacopeia requirements and provides advanced automation possibilities. FastTrack UV/VIS technology incorporates fibre optics with array detection and a Xenon flash lamp. The new spectrometers can be integrated with other laboratory equipment using LabX UV/VIS PC software for workflow control as well as advanced data analysis and management, compliant with 21 CFR part 11/EU annex 11.

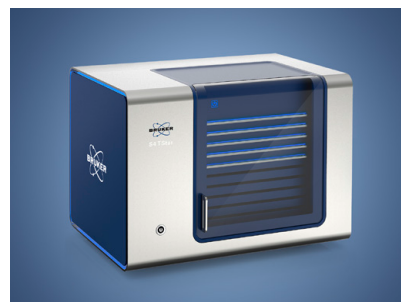
Bruker's S4 TStar total reflection XRF spectrometer has been designed for the requirements of increasingly regulated areas. It has up to three different X-ray excitation modes and the latest generation of the large area XFlash silicon drift detector. The automatic sample changer can handle 90 samples in up to 10 sample trays. Reduced internal air flow, special integrated sample housing and stackable storage boxes protect samples from contamination.



WITec's alpha300 access entry-level micro-Raman system can be upgraded



Mettler Toledo's UV/VIS Excellence range can easily be integrated with their other laboratory equipment



Bruker's TXRF spectrometer, the S4 TStar has been designed for use in regulated areas

Links for more information

To simplify your search for more information on products listed below, you can connect directly to the relevant product page for each product using the code number. If you are reading this in a printed copy, just put the number into your browser at the end of the URL string <http://link.spectroscopyeurope.com/28-03->. If you are reading this in a digital version, just click the links! Where a page is not currently available, we have provided a link to the company's home page or the most relevant page.

ATOMIC

- | | |
|--|-----------|
| 5110 ICP-OES is a new version of the 5100 with new software and integrated valve that can run a sample every 20 s (Agilent Technologies) | 50 |
| contrAA new generation of this series of continuum source atomic absorption spectrometers (Analytik Jena) | 51 |
| J200 tandem laser ablation and LIBS instrument (Applied Spectra) | 52 |

INFRARED

- | | |
|---|-----------|
| AIM-9000 infrared microscope system (Shimadzu) | 53 |
| Adulterant Screen software for FT-IR and NIR to perform authenticity and nutritional analysis in one step (PerkinElmer) | 54 |
| sFTIR no moving parts FT-IR which can measure at a modulation frequency of 50 Hz (Spectrolytic) | 55 |

MASS SPECTROMETRY

- | | |
|--|-----------|
| Autosampler for PTR-MS for VOC headspace analysis which can hold up to 270 vials of liquid, solid or gas samples (Ionicon) | 56 |
|--|-----------|

ANALYTICA 2016

CLAM-2000 fully automated sample preparation for liquid blood samples by LC-MS (Shimadzu)	57
HiPace 30 small turbopump capable of 32 L s ⁻¹ (Pfeiffer Vacuum)	58
HiPace 300 H turbopump specifically with high compression for light gases (Pfeiffer Vacuum)	59
MALDI PharmaPulse rapifleX label-free ultra-high throughput MALDI-TOF system (Bruker)	60
PesticideScreener solution based on Bruker's QTOF instruments with larger screening database (Bruker)	61
ToxScreener 2.1 running on Bruker's QTOF instruments with larger screening database (Bruker)	62
UHPLC-MS Biopharmaceutical Workflows include range of columns, instruments, software and consumables (Thermo Scientific)	63
xr Series family of thermal desorption instruments for GC-MS (Markes International)	64

NEAR INFRARED

AvaSpec-NIR256/512-2.5-HSC improved, compact NIR spectrometers with range of gratings available (Avantes)	65
PET analysis on MB3600 FT-NIR measuring % crystallinity, wall thickness and %H ₂ O (ABB)	66
Qred miniature NIR spectrometer with cooled InGaAs detector and customisable wavelength ranges up to 2500 nm (RGB Photonics)	67
Spec NIR: small, MEMS-based spectrometer with single element detector (Sarspec)	68

NMR

Minispec G-var time-domain NMR system for determination of droplet size in food emulsions (Bruker)	69
--	----

RAMAN

alpha300 access entry-level micro-Raman system for single-spot analysis and imaging (WITec)	70
alpha300 series has been overhauled increasing flexibility, sensitivity and speed (WITec)	71
Gemstones database of 365 Raman and 144 photoluminescence spectra of verified gemstones (ST Japan Europe)	72
Senterra II confocal, multi-laser Raman imaging microscope (Bruker)	73

SURFACE ANALYSIS

Esprit Qube software for 3D visualisation and post-processing of EBSD and/or ED XRF spectrometers on electron microscopes (Bruker)	74
--	----

TERAHERTZ

TeraScan Terahertz system with new digital control electronics (Toptica)	75
--	----

UV/VIS

FAbS double-beam spectrophotometer and fluorimeter combined (Sarspec)	76
S1S fibre-optic spectrometer (Sarspec)	77
UV/VIS Excellence is a new series of four models with fibre optics and array detection (Mettler Toledo)	78

X-RAY

Magpro 60kV 12W X-ray source for portable and benchtop instruments (Moxtek)	79
Cement-Quant ready-to-use solution for analysis of building materials (Bruker)	80
Geo-Quant M analysis solution for geology, mining and minerals (Bruker)	81
S4 TStar total reflection X-ray fluorescence spectrometer (Bruker)	82
Spectra.Elements software suite for the S2 Puma benchtop ED XRF spectrometer (Bruker)	83
Ultra-Lite Magnum 50kV X-ray source designed for handheld instruments (Moxtek)	84

Product Focus on Imaging Spectroscopy

Spectroscopy Europe Product Focuses highlight currently available instrumentation in a particular area of spectroscopy. This Product Focus is on Imaging Spectroscopy, and some companies have provided information on their key products, their applications and features.

See our media information (www.spectroscopyeurope.com/advertisers/media-packs) for details of future Product Focuses.

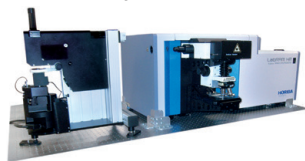
Nanophoton	Tel: 81-6-6878-9911
	info@nanophoton.jp
	http://www.nanophoton.jp

PRODUCT: Laser Raman Microscope RAMANtouch
APPLICATIONS: Pharmaceutical • Semiconductor • Polymer • 2D-material • Lithium-ion battery
KEY FEATURES: Diffraction-limited spatial resolution guaranteed for all users • Ultra-fast Raman imaging by line illumination • Fast and accurate laser beam scanning • High detection sensitivity of tiny particles less than 100 nm • high spectral resolution and high reproducibility

PRODUCT: Fast Screening System RAMANview
APPLICATIONS: Whole tablet Raman imaging • QA/QC of bulky samples • Fast Raman screening • QA/QC of large sheet samples • Raman imaging of samples in deep containers
KEY FEATURES: Ultra-wide field-of-view more than 800mm² • Extended depth of focus of up to about 1.4 mm • Unique working distance of more than 70 mm

HORIBA Scientific	Tel: 33 1 69 74 72 00	HORIBA Scientific
	info-sci.fr@horiba.com	
	www.horiba.com/raman	

PRODUCT: HR Evo Nano – AFM/Raman System
APPLICATIONS: 1D-2D Materials • Organic molecules • Polymers • Semiconductors • Photovoltaics
KEY FEATURES: TERS proven system • Raman excitation lines from DUV (229 nm) to NIR (1064 nm) • Ultra high spectral resolution • Fully automated operation • 1.3 μm AFM laser diode, top and side Raman-AFM optical coupling with high NA (up to 100×, 0.7NA) • Fast TERS mapping with SWIFTSX and EMCCD • Integrated software platform



PRODUCT: ParticleFinder for HORIBA Raman Microscopes
APPLICATIONS: Pharmaceuticals • Microplastics • Geology • Mineralogy
KEY FEATURES: Automatic detection of particles • Full characterisation of particles • Provides size, shape, number and chemical identification of particles • Complete solution for particle characterisation and identification

PRODUCT: TRIOS Platform – AFM and Optical Coupling Platform
APPLICATIONS: Materials sciences • Life sciences • Custom optical systems • Non-linear and near-field optics
KEY FEATURES: TERS imaging • Co-localised AFM-Raman imaging • Simultaneous optical access from the bottom with up to 1.4 NA oil immersion objective, from the top with up to 100× 0.7NA objective, from the side (optional) with up to 100× 0.7NA objective • Compatible with both XploRA and LabRAM HR Evolution spectrometers.

Daylight Solutions	Tel: +1-858-432-7500	DAYLIGHT SOLUTIONS® 
	jrowlette@daylightsolutions.com	
	www.daylightsolutions.com	

PRODUCT: Spero
APPLICATIONS: Label-free bio-imaging • Reaction dynamics • Microfluidics • Live cell studies • Materials and plasmonics
KEY FEATURES: High-brightness semiconductor infrared laser source • Real-time spectroscopic imaging capability • Complements and enhances mass spec techniques such as MALDI • Fits on a desktop and is easy to use • No cryogenic cooling required



WITec GmbH	Tel: +49(0)731 140 700	WITec focus innovations
	info@witec.de	
	www.witec.de	

PRODUCT: alpha300 R Confocal Raman Imaging System
APPLICATIONS: Materials research • Pharmaceuticals • Semiconductor and PV • Life Sciences • Geosciences
KEY FEATURES: Unmatched sensitivity and speed (0.76 ms/spectrum) • Confocal setup: highest spatial resolution (200 nm) and depth profiling • Acquires a complete Raman spectrum at each image pixel • 3D chemical imaging • Correlative Raman imaging easily possible: Raman-AFM, Raman-SNOM, TERS-ready

PRODUCT: apyron Automated Raman Imaging System
APPLICATIONS: Materials research • Pharmaceuticals • Forensics • Life science • Geoscience
KEY FEATURES: Push-button principle for high performance 3D Raman imaging • TruePower automated absolute laser power determination • Outstanding spectral and spatial resolution • Drastically reduced time required to become familiar with the operation of the instrument

PRODUCT: alpha300 access Confocal Micro-Raman System
APPLICATIONS: Surface analytics • Materials research • Life sciences • Quality control • Pharmaceuticals & biomedical research
KEY FEATURES: High-quality confocal-micro Raman spectroscopy • Single-spot & Raman mapping with exceptional spectral sensitivity • Specifically engineered for budget-conscious customers requiring superior performance • Access to the future of Raman spectroscopy through upgradeability

PRODUCT: TrueSurface Microscopy
APPLICATIONS: Large-area investigations • Characterisation of rough & inclined surfaces
KEY FEATURES: Topographic Raman Imaging • Confocal microscopy along with large area optical profiling • Precise tracing of the true surface while acquiring Raman imaging data • Generates images revealing chemical properties at the surface • Virtually no sample preparation of large samples

PRODUCT FOCUS

PRODUCT: RISE Microscopy – Raman SEM Imaging

APPLICATIONS: Materials research • Pharmaceuticals • Nanotechnology • Life science • Geoscience

KEY FEATURES: Correlative Raman-SEM imaging integrated in one system • Quick and convenient switching between Raman and SEM measurement: automated sample transfer from one measuring position to the other • Integrated software interface for user-friendly measurement control • Correlation of the measurement results and image overlay

Renishaw plc

 Tel: +44 (0) 1453 524524
raman@renishaw.com
www.renishaw.com/raman
PRODUCT: Renishaw's inVia™ Raman-SPM/AFM System

APPLICATIONS: Graphene • Materials sciences • Life sciences • Nanotechnology • Chemistry

KEY FEATURES: Reveals nanoscale chemical information • Produces nanoscale chemical maps • Provides simultaneous colocalised Raman and AFM data collection • Supports tip-enhanced Raman spectroscopy (TERS) and NSOM/SNOM • TERS mapping is complemented with high speed micro-Raman mapping

PRODUCT: Renishaw inVia™ Qontor® Confocal Raman Microscope

APPLICATIONS: Materials science • Semiconductors • Life sciences • Pharmaceuticals • Chemistry

KEY FEATURES: Ultra-high performance Raman microscope • Comprehensive suite of mapping and imaging techniques for 2D and 3D • kHz rate Raman spectra collection speeds • Real-time focus tracking generates images of uneven, rough and curved samples • Extensive range of accessories, laser, filter and mapping options

NEW PRODUCTS

IR detector

Hamamatsu Photonics has introduced the P13243 detector, using an InAsSb sensor as an eco-friendly alternative to lead salt. It provides high sensitivity over the 2.5–5.3 μm range with detectivity peaking at 1×10^9 (cmHz/W). The detectors are uncooled and so have low power consumption. Since they are photovoltaic, they require much simpler electronics.

Hamamatsu Photonics

▶ link.spectroscopyeurope.com/28-03-150

Handheld XRF analyser

Spectro Analytical Instruments have announced an upgrade of the Spectro xSort handheld X-ray fluorescence (XRF) spectrometer which improves speed and precision for light elements. It is available in various models. The xSort Alloy employs a silicon PIN detector and can provide grade identification of metals in seconds. The AlloyPlus has a silicon drift detector for high-productivity measurement and analysis.

Spectro Analytical Instruments

▶ link.spectroscopyeurope.com/28-03-151

Isotope ratio infrared spectrometer

The Thermo Scientific Delta Ray is a portable isotope ratio infrared spectrom-

eter for on-site isotopic analysis. Its URI Connect interface extends the continuous measurement of isotope ratios and concentrations of CO₂ in air to discrete samples, such as head space analysis or direct injection of small amounts of CO₂. By simultaneously detecting ¹³C and ¹⁸O, it can measure both isotopologues and concentration in one step without destroying the sample. The URI Connect system handles samples containing as little as 80 μg of CO₂.

Thermo Scientific

▶ link.spectroscopyeurope.com/28-03-152

Raman-SEM imaging broadens reach

WITec's RISE system for correlative Raman-scanning electron microscopy is now compatible with Zeiss' Merlin SEM. The combined system maintains all functions and features of a stand-alone Zeiss SEM and a WITec confocal Raman microscope. In Raman imaging mode the sample can be scanned through a range of 250 × 250 × 250 μm³. The microscope enables software-driven switching between Raman imaging and SEM, transformation of the Raman spectra into an image and the ability to overlay both images to produce the RISE image.

WITec

▶ link.spectroscopyeurope.com/28-03-153

NIR analysers

Unity Scientific has introduced the SpectraStar XT series of NIR spectrometers, adding many new technologies and components to the SpectraStar line. True Alignment Spectroscopy (TAS) is an instrument calibration and monitoring system for instrument calibration and validation. UScan routine operation software has a graphical, touchscreen drive interface for intuitive operation. There are a new controller board, InGaAs detector, grating drive motor and high-resolution encoder. There are models covering wavelength ranges between and up to 680–2600 nm. Ready-to-use pre-calibrated analysers are also available for many applications.

Unity Scientific

▶ link.spectroscopyeurope.com/28-03-154

Detector for nanosecond time-resolved imaging

Andor Technology has introduced the iStar sCMOS platform as an addition to the iStar family and offering frame rates >4000 fps, high sensitivity, high dynamic range, nanosecond gating and high-throughput fibre-optic coupling on an integrated unit with a high-resolution on-head digital delay generator.

Andor Technology

▶ link.spectroscopyeurope.com/28-03-155

Conferences 2016

19–24 June, Gothenburg, Sweden. **European Conference on X-Ray Spectrometry (EXRS2016)**. EXRS2016, Sweden MEETX AB, SE-412 94 Gothenburg, Sweden, ✉ exrs2016@meetx.se, ☞ <http://www.exrs2016.se>.

19–24 June, Ludwigsburg, Germany. **Spectroscopies in Novel Superconductors (SNS 2016)**. ☞ <http://www.fkf.mpg.de/SNS2016>.

19–24 June, Torun, Poland. **23rd International Conference on Spectral Line Shapes**. ✉ icls23@fizyka.umk.pl, ☞ <http://icls23.fizyka.umk.pl>.

20–24 June, Champaign-Urbana, Illinois, USA. **71st International Symposium on Molecular Spectroscopy**. Birgit D. McCall, International Symposium on Molecular Spectroscopy, University of Illinois, 306B Noyes Laboratory, 505 South Mathews Avenue, Urbana, IL 61801, USA. ✉ birgit@isms.illinois.edu, ☞ <http://isms.illinois.edu>.

26–30 June, Montreal, Canada. **SPEC 2016**. ☞ <http://www.spec2016.com>.

26–29 June, Inuyama, Japan. **7th International Workshop on Plasma Spectroscopy, IPS 2016**. ✉ ips2016@plasma.engg.nagoya-u.ac.jp, ☞ <http://www.ips2016inuyama.com>.

29 June–1 July, Groningen, The Netherlands. **8th International Conference on Coherent Multidimensional Spectroscopy (CMS 2016)**. ☞ <http://www.cms2016.org>.

3–7 July, Aarhus, Denmark. **EUROMAR 2016**. Prof. Thomas Vosegaard, Interdisciplinary Nanoscience Center and Department of Chemistry, Aarhus University, Denmark, ✉ tv@chem.au.dk, ☞ <http://euromar2016.org>.

3–6 July, Chamonix Mont-Blanc, France. **6th International Conference of the International Association for Spectral Imaging (IASIM 2016)**. ☞ <http://iasim16.sciencesconf.org>.

3–9 July, Dubrovnik, Croatia. **Mass Spectrometry in Biotechnology and Medicine (MSBM) Summer School**. ✉ msbm.dubrovnik@gmail.com, ☞ <http://www.msbm.org>.

4–6 July, Liverpool, UK. **18th Biennial National Atomic Spectroscopy Symposium (18th BNASS)**. ☞ <http://www.rsc.org/events/detail/19910>.

10–14 July, Stony Brook, New York, USA. **14th International Conference on Surface X-ray and Neutron Scattering (SXNS14)**.

Gretchen Cisco, ✉ sxns14@bnl.gov, ☞ <http://www.bnl.gov/sxns14>.

16–17 July, Biddeford, Maine, USA. **Gordon Research Seminar on Vibrational Spectroscopy**. ☞ <http://www.grc.org/programs.aspx?id=16690>.

17–22 July, Biddeford, Maine, USA. **Gordon Research Conference on Vibrational Spectroscopy**. ☞ <http://www.grc.org/programs.aspx?id=12221>.

17–22 July, Breckenridge, Colorado, USA. **58th Annual Rocky Mountain Conference on Magnetic Resonance**. ☞ <http://www.rockychem.com>.

17–22 July, Santa Fe, New Mexico, USA. **OSA Topical Meeting: International Conference on Ultrafast Phenomena**. ☞ http://www.osa.org/en-us/meetings/topical_meetings/international_conference_on_ultrafast_phenomena.

18–22 July, Mauritius. **International Conference on Pure and Applied Chemistry (ICPAC 2016)**. ✉ icpacmru@gmail.com, ☞ <http://sites.uom.ac.mu/icpac2016>.

19–21 July, Hamburg, Germany. **9th International Symposium on Environmental Analytical Chemistry (ISEAC39)**. Prof. Dr Jose Broekaert, University of Hamburg, Institut für Anorganische und Angewandte Chemie, Lehrstuhl für Analytische Chemie heterogener Systeme, Martin-Luther-King Platz 6, 20146 Hamburg, Germany. ✉ jose.broekaert@chemie.uni8hamburg.de, ☞ <http://www.iaec.com>.

24–27 July, Heidelberg, Germany. **28th International Symposium on Chiral Discrimination (Chirality 2016)**. Prof. Dr Oliver Trapp, Heidelberg University, Im Neuenheimer Feld 270, 69120 Heidelberg, Germany, ✉ info@chirality2016.com, ☞ <http://www.chirality2016.com>.

25–27 July, Glasgow, UK. **BSPR 2016: Proteomic Approaches to Health and Disease**. Karl Burgess, ✉ karl.burgess@glasgow.ac.uk, ☞ <http://www.bspr.org/node/527>.

25–28 July, Heidelberg, Germany. **OSA Optics and Photonics Congress: Imaging and Applied Optics**. ☞ http://www.osa.org/en-us/meetings/optics_and_photonics_congresses/imaging_and_applied_optics.

30 July–4 August, Szeged, Hungary. **33rd European Congress on Molecular Spectroscopy**. EUCMOS 2016 Secretariat, c/o Hungarian Chemical Society, Panna Korispataky, H-1015 Budapest, Hattyú u. 16. II/8, Hungary, ✉ eucomos2016@mke.org.hu, ☞ <http://eucomos2016.mke.org.hu>.

30 July–5 August, Chambersburg, Pennsylvania, USA. **18th International Diffuse Reflectance Conference (IDRC 2016)**. ☞ <http://www.idrc-chambersburg.org>.

1–5 August, Rosemont, Illinois, USA. **65th Annual Denver X-ray Conference (2016 DXC)**. ☞ <http://www.dxcicdd.com>.

14–19 August, West Dover, Vermont, USA. **Gordon Research Conference on Molecular Structure Elucidation**. ☞ <http://www.grc.org/programs.aspx?id=17262>.

14–19 August, Fortaleza, Brazil. **25th International Conference on Raman Spectroscopy (ICORS 2016)**. ☞ <http://www.icors2016.org>.

16–18 August, Campinas, Brazil. **The 6th IASTED International Conference on Modelling, Simulation and Identification—MSI 2016**. ✉ calgary@iasted.org, ☞ <http://iasted.org/conferences/cfp-840.html>.

20–26 August, Toronto, Canada. **21st International Mass Spectrometry Conference**. ✉ contact@imsc2016.ca, ☞ <http://www.imsc2016.ca>.

21–24 August, Los Angeles, California, USA. **8th Workshop on Hyperspectral Image and Signal Processing: Evolution in Remote Sensing (WHISPERS)**. ☞ <http://www.ieee-whispers.com>.

21–26 August, Kyoto, Japan. **International Conference on Magnetic Resonance in Biological Systems (ICMRBS XXVII)**. ✉ icmrbs2016@ics-inc.co.jp, ☞ <http://www.icmrbs2016.org>.

23–26 August, Moscow, Russia. **International Conference on Many Particle Spectroscopy of Atoms, Molecules, Clusters and Surfaces (MPS 2016)**. ✉ mps2016@sinp.msu.ru, ☞ <http://www.mps2016.ru>.

24–26 August, Reims, France. **14th Biennial HITRAN Database Conference & 13th Atmospheric Spectroscopy Applications (ASA) Meeting**. Maud Rotger, ✉ maud.rotger@univ.reims.fr, ☞ <http://www.univ-reims.fr/site/evenement/asa-hitran/home-accueil.18642.32042.html>.

26–28 August, Xi'an, China. **9th International Symposium on Photonics and Optoelectronics (SOPO 2016)**. ✉ sopo@sopoconf.org, ☞ <http://www.sopoc-onf.org/2016>.

28 August–2 September, Irkutsk, Russia. **Asia-Pacific EPR/ESR Symposium (APES 2016)**. Dr Dmitriy Polovyanenko, ✉ apes2016@nioch.nsc.ru, ☞ <http://www.apes2016.org>.

SPECTROSCOPY **READER SERVICE**

europa

Use this page to register for a free subscription to *Spectroscopy Europe*. You can also register online at the address below.

Online version at <http://www.spectroscopyeurope.com/register>

Your Details

Title (Professor/Dr etc.):	City:
First Name:	State/Region:
Last Name:	Postal Code:
Job Title:	Country:
Organisation Name:	E-mail:
Address:	

Please send me/continue to send me a free copy of *Spectroscopy Europe*. Signed: _____

Field of Work:

(please tick ALL that apply)

- Agriculture
- Analytical Chemistry
- Biotechnology
- Chemicals
- Electronics/Semiconductors
- Energy and Fuels
- Environmental
- Food
- Genomics and other -omics
- Instrumentation
- Life Science
- Materials Science
- Medical Sciences
- Metals and Minerals
- Nanotechnology
- Pharmaceuticals
- Polymers and Peptides
- Security and Forensics
- Water

Techniques:

(please tick ALL that apply)

- Atomic Absorption
- Atomic Emission
- Chemometrics
- Computers/Automation
- ICP/MS
- Infrared
- Laser Spectroscopy
- Luminescence/Fluorescence
- Mass Spectrometry
- Microscopy and Imaging
- MRI
- Near Infrared
- NMR, ESR, EPR
- Photonics and Optics
- Raman
- Separation Science
- Surface Analysis
- UV/Vis
- X-Ray Diffraction
- X-Ray Spectrometry
- None

Area of employment:

(please tick ONE only)

- Industry
- Independent Lab
- University/Institute
- Hospital
- Government
- Research Inst./Foundation
- Other _____

Job function: *(please tick ONE only)*

- Analyst
- Quality Control/Assurance
- Research Scientist
- Lab Manager
- University Professor
- Engineering/Design
- Manufacturing/Processing
- Teaching
- Marketing/Sales
- Other _____

Do you recommend, specify or authorise the purchase of spectroscopic instrumentation or services: Yes No

Your Personal Data (we will never pass your personal details to any third party)

John Wiley & Sons Ltd and IM Publications LLP will use the information you have provided to fulfil your request. In addition, we would like to:

1. Contact you by post with information and offers from relevant companies (your details are never disclosed to them). Tick here if you do NOT want to receive this:
2. Contact you by e-mail with information and offers from relevant companies (your e-mail address and details are never disclosed to them). Tick if you WANT to receive this:
3. Your registration to this website includes a regular e-mail newsletter alerting you to the latest content. Tick if you do NOT want to receive this:

Now fax this page to +44-1243-811711, or return by mail to: *Spectroscopy Europe*, 6 Charlton Mill, Charlton, Chichester, West Sussex PO18 0HY, UK.

28 August–1 September, San Diego, California, USA. **SPIE Optics + Photonics**. <http://spie.org/x30582.xml>.

30 August–3 September, Prague, Czech Republic. **24th International Conference on High Resolution Molecular Spectroscopy (PRAHA2016)**. Professor Štěpán Urban, University of Chemistry and Technology, Faculty of Chemical Engineering, Technická 5, CZ-16628 Praha 6, Czech Republic, ✉ paha16@vscht.cz, <http://www.chem.uni-wuppertal.de/conference>.

31 August–2 September, Edinburgh, UK. **Ultra Fast Imaging of Photochemical Dynamics**. <http://www.rsc.org/events/detail/19765>.

4–8 September, Torino, Italy. **10th Conference of the European Federation of EPR Groups (EFEPR)**. ✉ efepr2016@unito.it, <http://www.efepr2016.unito.it>.

4–9 September, Bayreuth, Germany. **54th European High Pressure Research Group International Meeting (EHPRG 2016)**. <http://www.ehprg2016.org>.

4–8 September, Potchefstroom, South Africa. **International Symposium on the Industrial Applications of the Mössbauer Effect (ISIAME 2016)**. Prof. Frans Waanders, ✉ frans.waanders@nwu.ac.za, http://www.medc.dicp.ac.cn/news/201512/20151208_30000025.php?id=30000025.

5–8 September, Leeds, UK. **Photon16**. Joanne Hemstock, ✉ joanne.hemstock@iop.org, <http://www.photon.org.uk/home>.

6–9 September, Shenzhen, Guangdong, China. **18th China International Optoelectronic Expo (CIOE 2015)**. <http://www.cioe.cn/EN>.

11–14 September, Dresden, Germany. **20th European Symposium on Polymer**

Spectroscopy. <http://www.ipfdd.de/ESOPS20>.

11–14 September, La Jolla, California, USA. **SMASH 2016: Small Molecule NMR Conference**. <http://www.smashnmr.org>.

11–16 September, Antwerp, Belgium. **5th International Conference on Vibrational Optical Activity**. Prof. Dr Christian Johannessen, University of Antwerp, Groenenborgerlaan 171, B-2020 Antwerp, Belgium, ✉ voa5@uantwerpen.be, <http://www.voa5.org>.

11–15 September, Seville, Spain. **6th EuCheMS Chemistry Congress**. <http://euchems-seville2016.eu>.

12–16 September, Chamonix-Mont Blanc, France. **9th International Conference on Laser Induced Breakdown Spectroscopy (LIBS 2016)**. Conference office, Université Claude Bernard Lyon 1, Cellule Congrès de l'UCBL, LIBS 2016, 43, bd du 11 Novembre 1918, 69622 Villeurbanne Cedex, France. ✉ contact@libs2016-france.org, <http://www.libs2016-france.org/en>.

13–15 September, Eastbourne, UK. **37th Annual Meeting of the British Mass Spectrometry Society (BMSS 2016)**. <http://www.bmss.org.uk/meetings.shtml>.

18–23 September, Santa Fe, New Mexico, USA. **2016 SciX Conference (formerly FACSS)**. ✉ facss@facss.org, <http://www.facss.org>.

18–21 September, Dallas, Texas, USA. **130th AOAC International Meeting and Exposition**. <http://www.aoac.org>.

19–22 September, Warsaw, Poland. **European Materials Research Society (E-MRS) 2016 Fall Meeting**. Marek Godlewski, Institute of Physics, Polish Academy of Sciences, Al. Lotników 32/46 02-668, Warszawa, Poland, ✉ [\[ifpan.edu.pl\]\(mailto:ifpan.edu.pl\), <http://www.european-mrs.com/meetings/2016-fall>.](mailto:godlew@</p>
</div>
<div data-bbox=)

25–30 September, Copenhagen, Denmark. **41st International Conference on Infrared, Millimeter and Terahertz Waves (IRMMW-THz 2016)**. <http://www.irmmw-thz2016.org>.

26–28 September, Ulm, Germany. **13th Confocal Raman Imaging Symposium**. Dr Karin Hollricher, WITec GmbH, Lise-Meitner-Str. 6, 89081 Ulm, Germany, ✉ Karin.Hollrichr@witec.de, <http://www.witec.de>.

Courses 2016

13–16 June, Todi, Italy. **Multivariate Analysis Course, School for Novices**. <http://www.cma4ch.org/frames-cou.html>.

13–17 June, Warwick, UK. **Interpretation of Infrared and Raman Spectra**. James A. de Haseth, IR Courses, Inc. 165 Sunnybrook Drive, Athens, Georgia 30605-3347, USA, ✉ dehaseth@ircourses.org, <http://www.ircourses.org/schedUK.html>.

16–17 June, Milton Keynes, UK. **2-day The GC & GC-MS Clinic**. <http://www.anthias.co.uk/training-courses/GC-clinic>.

23–25 November, Utrecht, Netherlands. **Multivariate Analysis Of Spectroscopic Data**. <http://www.camo.com/training/more/en/spectroscopy.html?id=726&tid=20&po=1>.

Exhibitions 2016

11–15 September, Seville, Spain. **6th EuCheMS Chemistry Congress**. <http://euchems-seville2016.eu>.

ADVERTISERS INDEX

Amptek.....	3
Bibby Scientific/Jenway.....	27
Bruker.....	11, 15, 19
Jeol.....	2
IM Publications.....	13
Shimadzu.....	5
Starna Scientific.....	21

Read *Spectroscopy Europe* wherever, whenever you want!



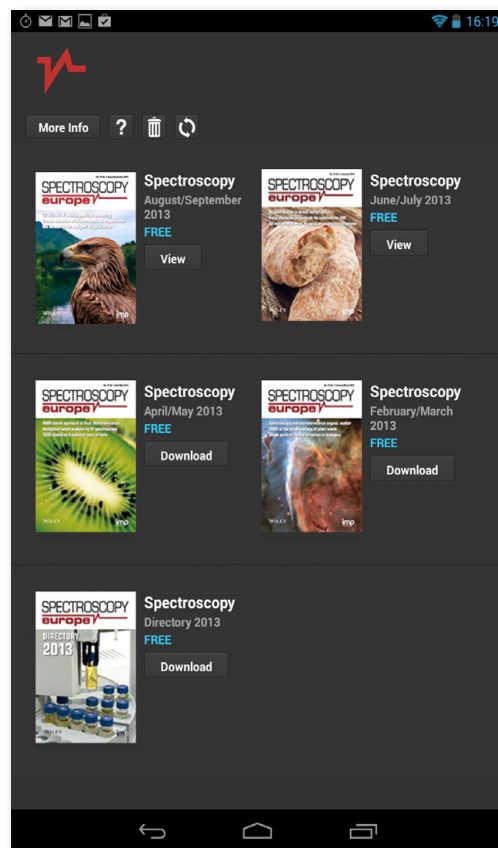
Spectroscopy Europe's new Apps are available free-of-charge for both Apple and Android devices, and can be read on tablets and phones. So you can catch up with all our great content wherever you are and whenever you want.

Download from the App Store or Google Play—just search for “spectroscopy europe”.

All the 2015 to 2013 back issues are already available to you when you install the App. Accept notifications from us, and you will know as soon as the latest issue is available.

We now offer you many ways to read *Spectroscopy Europe*: in print and digital editions, online at www.spectroscopyeurope.com and now on Apple and Android devices. And all are totally free-of-charge.

Download your App today.



Apple is a trademark of Apple Inc., registered in the U.S. and other countries. App Store is a service mark of Apple Inc. Google Play is a trademark of Google Inc.

www.spectroscopyeurope.com/apps